The Helicase-Like transcription factor synergizes with HTLV-1 TAX to activate the NF-¿B Pathway

Auteur : Sare, Ramatou
Promoteur(s) : Beauvois, Aurélie
Faculté : Gembloux Agro-Bio Tech (GxABT)
Diplôme : Master en bioingénieur : chimie et bioindustries, à finalité spécialisée
Année académique : 2021-2022
URI/URL : http://hdl.handle.net/2268.2/15271

LIÈGE université
Gembloux
Agro-Bio Tech

THE HELICASE-LIKE TRANSCRIPTION FACTOR SYNERGIZES WITH HTLV-1 TAX TO ACTIVATE THE NF-KB PATHWAY

SARE RAMATOU

TRAVAIL DE FIN D'ÉTUDES PRÉSENTÉ EN VUE DE L'OBTENTION DU DIPLÔME DE MASTER BIOINGÉNIEUR EN CHIMIE ET BIO-INDUSTRIE

ANNÉE ACADÉMIQUE 2021-2022

(CO)-PROMOTEUR(S): AURELIE BEAUVOIS AND LUC WILLEMS

[1]Dans ce cas, l'autorité académique est représentée par le(s) promoteur(s) membre du personnel(s) enseignant de GxABT

LIÈGE université
Gembloux
Agro-Bio Tech

THE HELICASE-LIKE TRANSCRIPTION FACTOR SYNERGIZES WITH HTLV-1 TAX TO ACTIVATE THE NF-KB PATHWAY

SARE RAMATOU

TRAVAIL DE FIN D'ÉTUDES PRÉSENTÉ EN VUE DE L'OBTENTION DU DIPLÔME DE MASTER BIOINGÉNIEUR EN CHIMIE ET BIO-INDUSTRIE

ANNÉE ACADÉMIQUE 2021-2022

(CO)-PROMOTEUR(S): AURELIE BEAUVOIS AND LUC WILLEMS

Home institution

This master's thesis has been conducted in the laboratory of Cellular and Molecular Epigenetics, located in the research center GIGA-cancer (the University of Liege, Belgium). This center offers a remarkable pooling of logistic, technical, and administrative resources, allowing research of high quality.

Acknowledgments

This Master's thesis is the result of six and a half months of research work carried out in a very enriching framework for me, from a personal and professional point of view. I would like to thank all the people with whom I had the opportunity to interact and who helped me to complete this master's thesis.

First, I would like to thank my academic supervisor, Professor Luc Willems, for giving me the opportunity to do my thesis in his laboratory. I would also like to thank him for his availability and especially his judicious advice which contributed to the accomplishment of this project.

Then, I would like to thank my laboratory supervisor, Aurélie Beauvois, who shared her knowledge and experience acquired in research. She was also able to give me her confidence and a large independence in the accomplishment of the various experiments carried out. I would like to thank her above all for her immeasurable kindness, her patience, her availability, for having re-read and corrected my thesis. Her writing advice was very valuable.

I would also like to thank the whole laboratory team of the epigenetic cell: Malik Hamaidia, Majeed Jamakhani, Hélène Brossel, Mégane Willems, Julie Radermecker, Alexis Fontaine, Louise Halkin and Mélanie Grégoire for their presence in the laboratory.

Finally, I would like to express my sincere thanks to my family: my mother, my grandmother and all my relatives and friends, who accompanied, helped, supported, and encouraged me throughout the realization of this thesis.

Abstract

The human T-cell leukaemia virus type 1 (HTLV-1) is the first human retrovirus that has been discovered. It induces serious diseases including the adult T-cell leukaemia (ATL) and the HTLV-1-associated myopathy/tropical spastic paraparesis (HAM/TSP). Approximately 20 million people worldwide are infected with this oncogenic retrovirus, but only 5-10% will develop disease related to the infection. Tax, a trans-regulatory, activating nuclear oncoprotein, encoded by HLTV-1, has been identified as essential for cell replication and transformation. Preliminary data have shown that the helicase-like transcription factor (HLTF), a DNA damage tolerance regulator, is a restriction factor able to reduce HTLV-1 infectivity. These studies also demonstrated that HLTF interacts with Tax.

The objective of this undergraduate thesis is to evaluate the impact of Tax and HLTF on transcriptional activity directed by the HLTF promoter and the HTLV-1 long terminal repeat (LTR). Activation of the NF-κB pathway will also be evaluated in presence of wild-type and mutants of HLTF and Tax.

Data show that Tax mutants defective in NF-κB activation are expressed at lower levels compared to wild-type Tax. Luciferase reporter assays further show that Tax and HLTF mutants do not impact HLTF promoter activity. HLTF mutants do influence neither the transcription directed by the LTR nor the NF-κB pathway. Simultaneous induction of Tax and HLTF produces a synergistic effect on a NF-κB-AP-1-Luc reporter.

In summary, this work contributed to a better understanding of the mechanisms involved in the interactions between Tax and HLTF.

Keywords: HTLV-1, HLTF, NF-κB, restriction factors, transcription factor

Résumé

Le virus de la leucémie humaine à cellules T de type 1 (HTLV-1) est le premier rétrovirus humain découvert. Il induit plusieurs pathologies dont la leucémie à cellules T de l'adulte (ATL) et la myélopathie associée au HTLV-1/paraparésie spastique tropicale (HAM/TSP). Environ 20 millions de personnes dans le monde sont infectées par ce rétrovirus oncogène mais uniquement 5 à 10% vont développer des pathologies liées à l'infection. Tax, une oncoprotéine nucléaire trans-régulatrice, activatrice codée par HLTV-1, été identifiée comme étant essentielle pour la réplication et la transformation cellulaire. Des données préliminaires ont démontré que le facteur de transcription de type hélicase (HLTF), un régulateur de tolérance aux dommages à l'ADN est un facteur de restriction, capable de réduire l'infectivité de HTLV-1. Ces études ont également démontré que HLTF interagit avec Tax.

L'objectif de ce projet est d'évaluer l'impact de Tax et d'HLTF lors de l'induction simultanée de ces deux protéines (Tax et HLTF) sur l'activation la longue répétition terminale (LTR) du HTLV-1, de la voie d'activation de NF-κB et du promoteur HLTF.

Nos données démontrent que les mutants défectifs pour l'activation de NF-κB sont exprimés à des niveaux moindres. Les essais rapporteurs luciférase montrent également que les mutants de Tax et d'HLTF n'influencent pas l'activité du promoteur d'HLTF. Des mutants d'HLTF n'impactent ni la transcription dirigée par le LTR ni la voie NF-κB. L'induction simultanée de Tax et HLTF produit un effet synergique sur un rapporteur NF-κB-AP-1-Luc.

En conclusion, notre travail a contribué à une meilleure compréhension des mécanismes impliqués dans les interactions entre Tax et HLTF.

Mots-clés : HTLV-1, HLTF, NF-κB, facteurs de restriction, facteur de transcription

List of acronyms

AMP	Adenosine Monophosphate
ANK	Ankyrin Repeat
ANOVA	Analysis Of Variance
AP-1	Activator Protein-1
ATF/ CREB	Activating Transcription Factors/ Cyclic AMP-Responsive Element Binding Protein
ATL	Adult T-Cell Leukaemia
ATP	Adenosine Triphosphate
BAFF	B-Cell Activating Factor
BCA	Bicinchoninic Acid
BLV	Bovine Leukaemia Virus
BSA	Bovine Serum Albumin
bZIP	Leucine Zipper
CBP	CREB Binding Protein
cDNA	Complementary DNA
CREB	Cyclic AMP-Responsive Element Binding Protein
DBD	DNA-Binding Domain
DC	Dendritic Cell
DD	Death Domain
DMEM	Dulbecco's Modified Eagle Medium
DNA	Deoxyribonucleic Acid
Dox	Doxycycline
EGFP	Enhanced Green Florescent Protein
Env	Envelope Protein
FBS	Fetal Bovine Serum
GAPDH	Glyceraldehyde-3-Phosphate Hydrogenase
GEO	Gene Expression Omnibus (NCBI)
GLUT-1	Glucose Transporter
GRR	Glycin-Rich-Region
HAM	HTLV-1 Associated Myelopathy
HBZ	Htlv-1 Basic Leucine Zipper

HCMV	Human Cytomegalovirus
HIRAN	HIP116 Rad5p N-Terminal
HIV	Human Immunodeficiency Virus
HLTF	Helicase-Like Transcription Factor
HLTV-1	Human T-Cell Leukaemia Virus Type 1
HPRT	Hypoxanthine Phosphoribosyltransferase
IKK	IκB Kinase Complex
LPS	Lipopolysaccharides
LR	Leucine-Rich Sequence
LRR	Leucine Repeat Region
LTR	Long Terminal Repeat
Luc	Luciferase
LZ	Leucine Zipper
MRNA	Messenger RNA
MTOCs	Microtubule Organization Centers
NCBI	National Center for Biotechnology Information
NEMO	NF-κB Essential Modulator
NES	Nuclear Export Signal
NF-κB	Nuclear Factor Kappa-Light-Chain-Enhancer of Activated B Cells
NIH	National Institutes of Health
NIK	NF-κB-Inducing Kinase
NLS	Nuclear Localization Signal
NRP-1	VEGF-165 Receptor Neuropilin-1
O/N	Overnight
PBS	Phosphate Buffered Saline
PCR	Polymerase Chain Reaction
PEI	Polyethyleneimine
PEST	Proline-, Glutamic Acid-, Serine-, And Threonine-Rich Region
PTLV	Primate T-Lymphotropic Virus
RHD	Rel Homology Domain
RING	Really Interesting New Gene
RIPA	Radioimmunoprecipitation Assay

RLU	Relative Light Units
RNA	Ribonucleic Acid
RT	Room Temperature
RT-qPCR	Real Time Polymerase Chain Reaction Using Reverse Transcription
SDS	Sodium Dodecyl Sulfate
SNF2	Sucrose Non-Fermenting 2
SRF	Serum Response Factor
STLV	Simian T-Lymphotrophic Virus
SWI/SNF	Switch/Sucrose Non-Fermenting
TAD	Transcription Activation Domain
TAK1	TGF-Beta Kinase 1
Tax	Transactivator of the pX Region
TBST	Tris Buffered Saline with Tween
TGF	Transforming Growth Factor-Beta Activated Kinase 1
TIGIT	T Cell Immunoreceptor with Ig and ITIM Domains
TM	Transmembrane Protein
TNF	Tumor Necrosis Factor
TRE	Tax-Responsive Elements
TREF3	TNF Receptor-Associated Factor 3
TSP	Tropical Spastic Paraparesis
UTR	Untranslated Region
UV	Ultraviolet
VS	Virological Synapse
VSV	Vesicular Stomatitis Virus
WT	Wild Type
YFP	Yellow Fluorescent Protein

Table of figures

Table of contents

I) State of art

1) HTLV-1

Human T-cell leukemia viruses (HTLVs), belonging to the primate T-lymphotropic virus (PTLV) family, are complex retroviruses[1]. Human T-cell leukemia virus type 1 (HTLV-1) or T-lymphotrophic virus type 1 is a member of the deltaretrovirus family, which includes the simian T-lymphotrophic virus (STLV) and bovine leukemia virus (BLV). HTLV-1, HTLV-2, HTLV-3, and HTLV-4 are the four known strains of HTLV identified. HTLV-1 and HTLV-2 are prevalent worldwide[2]. The HTLVs are thought to derive from interspecies transmission between monkeys and humans. The genetic variation among HTLV-1 strains is less than 8%, and HTLV-1 and HTLV-2 show 70% nucleotide homology[2,3]. The discovery of HTLV-1 proceeded rather independently in Japan and the United States.

HTLV-1 was the first retrovirus isolated in a T-cell line derived from a patient with cutaneous T-cell lymphoma in 1980 and was shown to be the etiological agent of adult T-cell leukemia (ATL)[2,4,5]. Approximately 90% of the infected individuals remain asymptomatic carriers during their lives[6]. Around 5 to 10% of the HTLV-1 infected patients will develop serious diseases[7]. The most important HTLV-1-associated diseases are ATL, a very aggressive form of leukemia, and the HTLV-associated myelopathy/tropical spastic paraparesis (HAM/TSP), a neurological demyelinating disease[1]. ATL is a very aggressive disease characterized by lymphadenopathies, hepatoslenomegaly, visceral lesions (lung, skin), paraneoplastic hypercalcemia and the presence of leukemic cells with multilobulated nuclei (florid cells) (**Figure 1**)[8]. This disease is resistant to chemotherapy, leading to a mean survival time of only a few months[5]. HTLV-1 is also associated with inflammatory diseases including immunosuppression, polymyositis, alveolitis, mononeuropathy, infectious dermatitis in children and uveitis[5,9].

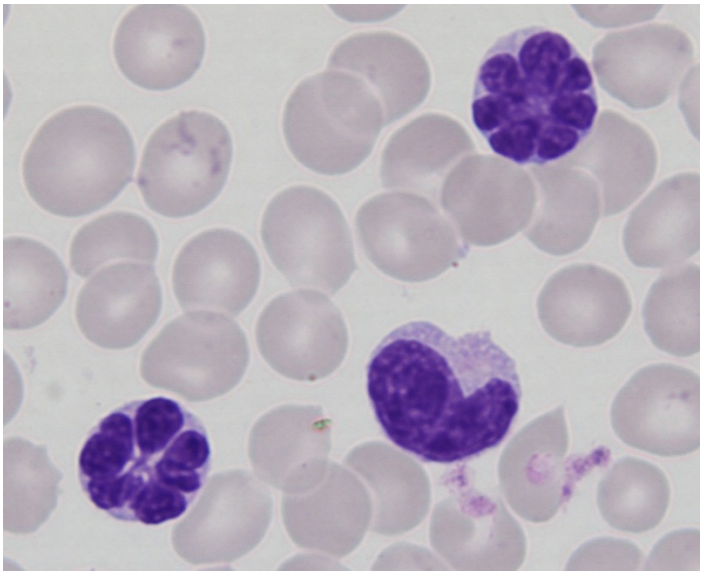

Figure 1: Typical "flower cell", leukemic cells with multilobulated nuclei in the peripheral blood of an acute ATL patient[8]

2) Epidemiology

Several studies were initiated both by American and Japanese researchers, very rapidly after HTLV-1 discovery and its association with ATL, to get insights into the distribution, the transmission modes, as well as the origin of HTLV-1[10]. HTLV-1 is not a ubiquitous virus. Although it is difficult to know the exact number of people infected worldwide, it is currently estimated to be around 10-20 million[7,11,12]. Major foci of endemic infection with HTLV-1 are located in southwestern Japan, the Caribbean, Central and South America, intertropical Africa, certain regions of Melanesia, India, the Middle East (north-eastern Iran)[2,5,11]. There are also smaller foci in the aboriginal populations of Australia, Papua New Guinea, and northern Japan[9](**Figure 2**).

There are several subtypes of HTLV-1 (subtypes A to G), depending on nucleotides variety, They all have a similar pathogenic potential[11,13]. The Cosmopolitan subtype A, the Central African subtype B, the Central African/Pygmies subtype D, and the Australo-Melanesian subtype C are the four major geographic subtypes (genotypes) that have been reported. About rare subtypes (E, F, G), a limited number of strains are found in Central Africa. The Cosmopolitan subtype A which is the most widespread subtype comprises several geographical subgroups. It is endemic in Japan, the Caribbean area, Central and South America, North and West Africa as well as part of the Middle East. A relatively recent dissemination (some centuries to few millennium) of this genotype from a common ancestor could explain the low sequence variability within subtype A. The most divergent is the Australo-Melanesian subtype

C. The appearance of these HTLV-1 subtypes in humans was strongly thought to be linked to interspecies transmission between STLV-1 infected monkeys and humans, followed by variable period of evolution in the human host[10] (**Figure 2**).

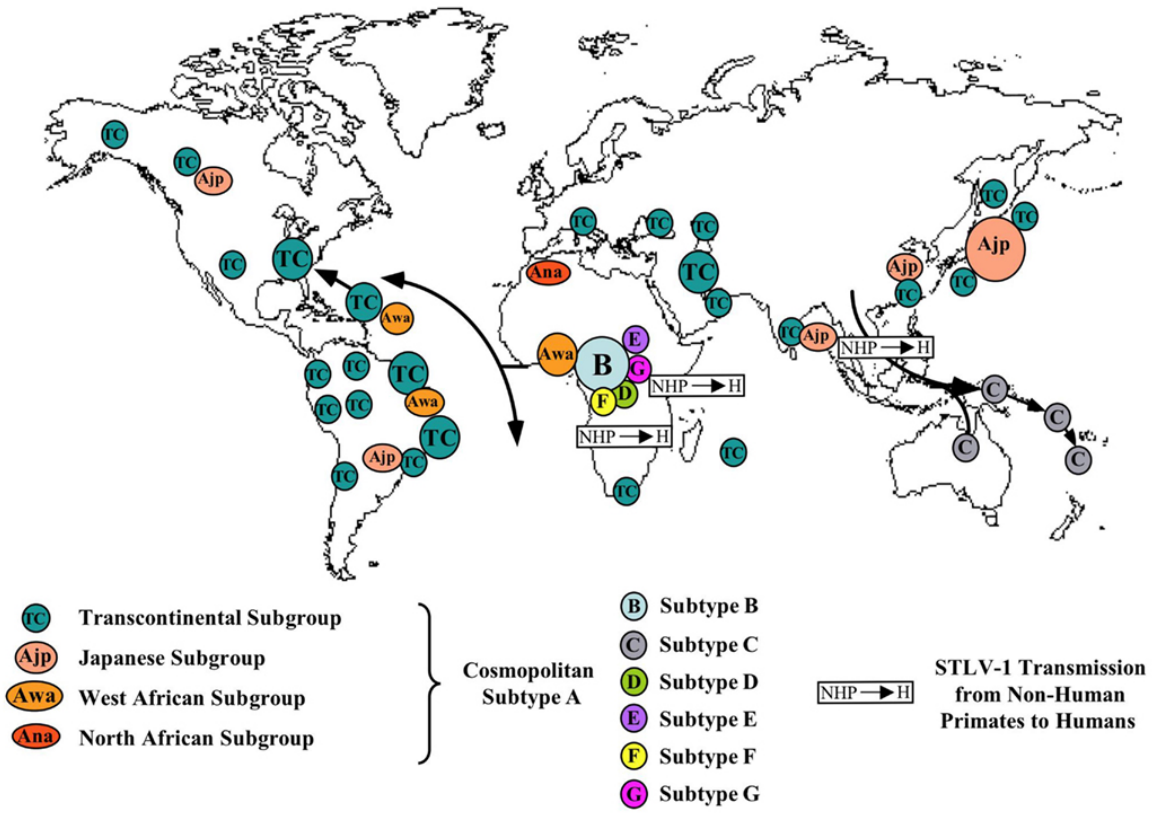

Figure 2: Map of geographical distribution of HTLV-1 subtypes (A–G), and the main modes of viral dispersion through movement of infected populations[14]

3) Transmission and treatment

Being the first retrovirus discovered, HTLV-1 contributed to the rapid identification of Human Immunodeficiency Virus (HIV) in 1983. This fact, both retroviruses share the same transmission routes[4]. HTLV-1 is transmitted through three major routes by breastfeeding from mother to child, sexual contact and needle sharing specially drug users which mediates exposure to contaminated blood[10,15,16].

The predominant transmission mode in the endemic areas is mother-to-child. This mother-to-child transmission is mainly linked to a prolonged breastfeeding after 6 months of age[17]. About 15-25% of children of HTLV-1 infected mothers will become infected, mostly through the milk due to the presence of infected cells, but for only 5% transplacentally[5,18]. Lifetime sexual transmission rates between partners are 60% from infected males to females and only 0.4% from infected females to males. This transmission is possible due to the presence of HTLV-1 in genital secretions[17]. Sexual transmission of HTLV-1 requires entry through mucosal barriers in the female and male genital tracts. As during transmission by breastfeeding, the virus can be transmitted where lesions disrupt the mucosa, by infection of the epithelium or by transcytosis across epithelial cells[19]. More recently in the human population, HTLV-1 is also transmitted through the bloodstream during transfusion of blood components containing infected T-cells. HTLV-1 transmission by the transfusion of cellular blood components, results in seroconversion in more than 10-50% of recipients[11]. Transmission by blood transfusion can potentially be eliminated by screening of blood donations, as practiced in Japan, the United States, France, and some islands of the West Indies, although the cost would be prohibitive in other endemic areas[5]. HTLV-1 can also be transmitted in intravenous drug users, again via infected lymphoid cells[11,20].

4) Structure of the virus

a) Structure of the virion

HTLV-1 is an enveloped virus of approximately 100nm in diameter[21]. The virion envelope exhibits a proteolipid envelope bilayer of host cell membrane origin, which has viral transmembrane and surface proteins. The icosahedral capsid enables protection of the viral RNA and the viral enzymes (functional protease, reverse transcriptase, and integrase), while the inner envelope contains the matrix layer (**Figure 3A**)[21].

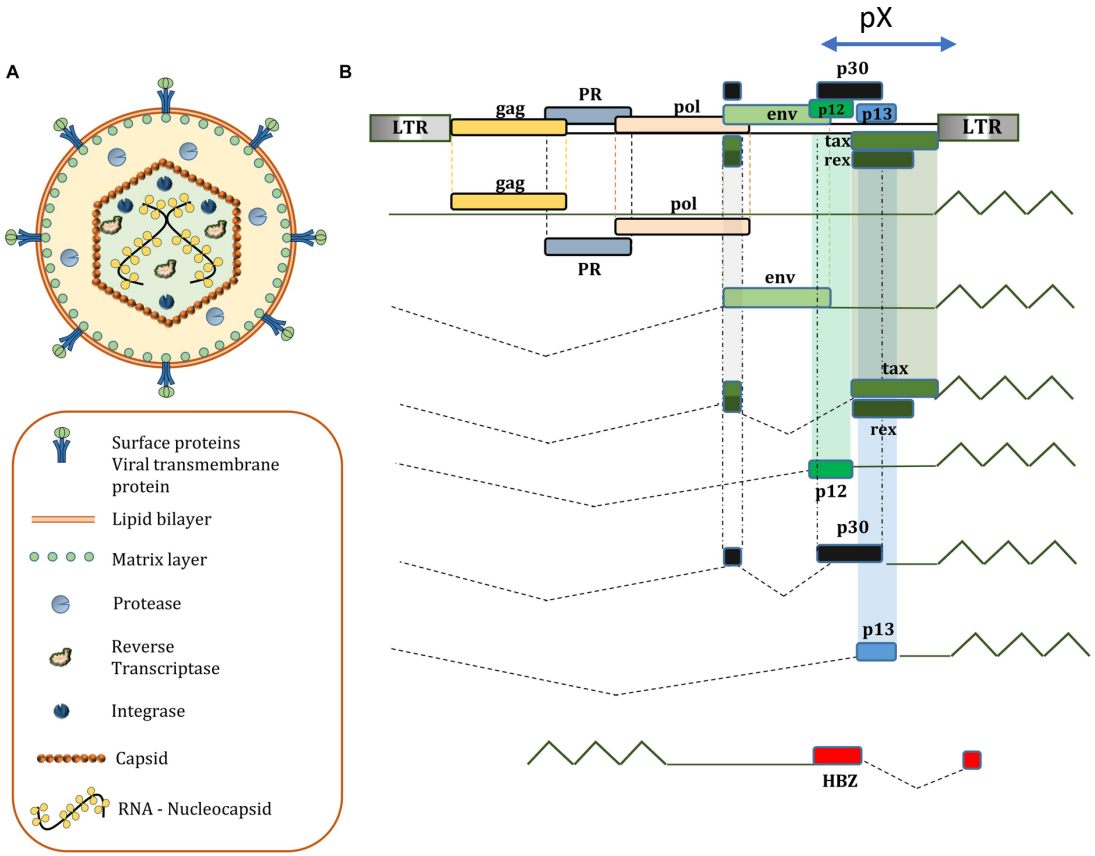

Figure 3: (A) Structure of a mature HTLV-1 virion; (B) Structure of the viral genome of HTLV-1[22].

b) Structure of the viral genome

The genomic structure of the HTLV-1 virus consists of two long terminal repeats (LTRs) at the 3' end (3'LTR) and the 5' end (5'LTR) containing the viral promoter and regulatory elements (**Figure 3B**). The 5′ LTR is the promoter for the transcription in the sense orientation, whereas the 3′ LTR is the promoter for the antisense transcription[23]. Like other retroviruses, HTLV-1 carries a single-stranded RNA genome of approximately 9kb encoding for structural and enzymatic proteins, gag, pro, env, and pol [24,25]. In addition to structural genes (gag, pol and env), HTLV-1 contains regulatory genes (Tax and rex) and accessory genes such as p12, p13, p30 and HBZ in four overlapping open reading frames located in the pX region of the viral genome (**Figure 3B**)[26]. These proteins (Tax, rex, p12, p13, p30, HBZ) have been implicated to play a role in viral persistence[27]. The pX region is a unique region between the env terminator and the 3' LTR of the integrated proviral genome which encodes several regulatory and accessory genes on both the sense and antisense genomic strands[25,28].

Oncoprotein Tax is a well-characterized oncogenic viral protein and works as a transactivator of HTLV-1 5′ LTR. It is encoded in the pX region in the sense orientation[29]. Tax modulates the

transcription of numerous cellular genes involved in cell proliferation and differentiation, cell cycle control and DNA repair[30,31]. Tax is thus essential for HTLV-1 transformation of primary human T-cells[32,33].

The oncoprotein HBZ is also encoded in the pX region, but in the anti-sense orientation. HBZ modulates both viral and cellular gene transcription by interacting with cellular factors JunB, c-Jun, JunD, cAMP response element binding (CREB), and CREB binding protein (CBP)/p300[34,35]. HBZ also plays a crucial role in T-cell proliferation[36]. HBZ acts as a repressor of Tax-induced viral transcription by forming heterodimers with the transcription factor CREB-2 that are no longer able to bind to the viral CREB and thus consequently are no longer able to activate the 5'LTR HTLV-1 promoter[37]. These two oncoproteins Tax and HBZ are implicated in oncogenesis induced by HTLV-1[23].

5) Infection

HTLV-1 replicates mainly through clonal expansion of the infected cells rather than cell-free virus infection and it causes a persistent infection in humans. Cell-free viral infection is extremely ineffective, viral transmission mainly occurs in a cell-to-cell mediated manner [19].

HTLV-1 is detected originally in CD4+ T-cells but can infect a wide range of human cell types in vivo, including CD8+ T-cells, B cells, monocytes, macrophages, endothelial cells, and dendritic cells[27,38,39]. Since HTLV-1 is predominantly found in CD4+ T-cells in vivo, it is considered a T-cell tropic virus[40,41]. This distinct tropism results in post-infection T-cell proliferation as well as clonal expansion of virally infected CD4+ T-cells[42].

a) Virological synapse

The specialized area of cell-to-cell contact induced by HTLV-1 virus that promotes the directed transmission of the virus between cells is called virological synapse (VS). Many viruses spread efficiently by cell-to-cell contact. Contact between an infected cell and another uninfected cell is actively induced by VS (**Figure 4**)[43]. When this occurs, viral Gag and Env proteins and genomic RNAs are redirected to the point of contact between the infected and uninfected T-cells[19]. A good indication of the establishment of a VS is the polarization of the Microtubule Organization Centers (MTOCs) of the infected cell towards the cell contact formed with the target cell[43,44].

b) Cellular conduits

Cellular conduits allow the transmission of HTLV-1 virus over long distances[45]. This transmission occurs by the spread of HTLV-1 virus from an infected T-cell to an uninfected T-cell via membrane extensions (**Figure 4**). HTLV-1 particles are concentrated between the conduits because this transmission (cellular conduits) takes place during VS formation: this was revealed and demonstrated by transmission electron microscopy[19]. The accessory protein p8 in HTLV-1 infected cells increased the number and length of the conduits as well as the number of contacts between infected and uninfected cells, thus enhancing communication between different cell types[19,46,47].

c) Viral biofilm

Biofilms are also a mode of cell-to-cell transmission of HTLV-1. This mode of transmission is used by virions to hide from the immune system and spread within the host. At the level of the plasma membrane, these HTLV-1 virions bud[48]. These buds are temporarily embedded in adhesive extracellular structures rich in carbohydrates, collagen, galectin-3 and tetherin (binding proteins), O-glycosylated surface receptors (CD43, CD45)[45,48]. These viral biofilms are therefore related to bacterial biofilms. Infection is thus promoted by these extracellular viral assemblies which adhere rapidly to cell contacts with other lymphocytes[48] (**Figure 4**).

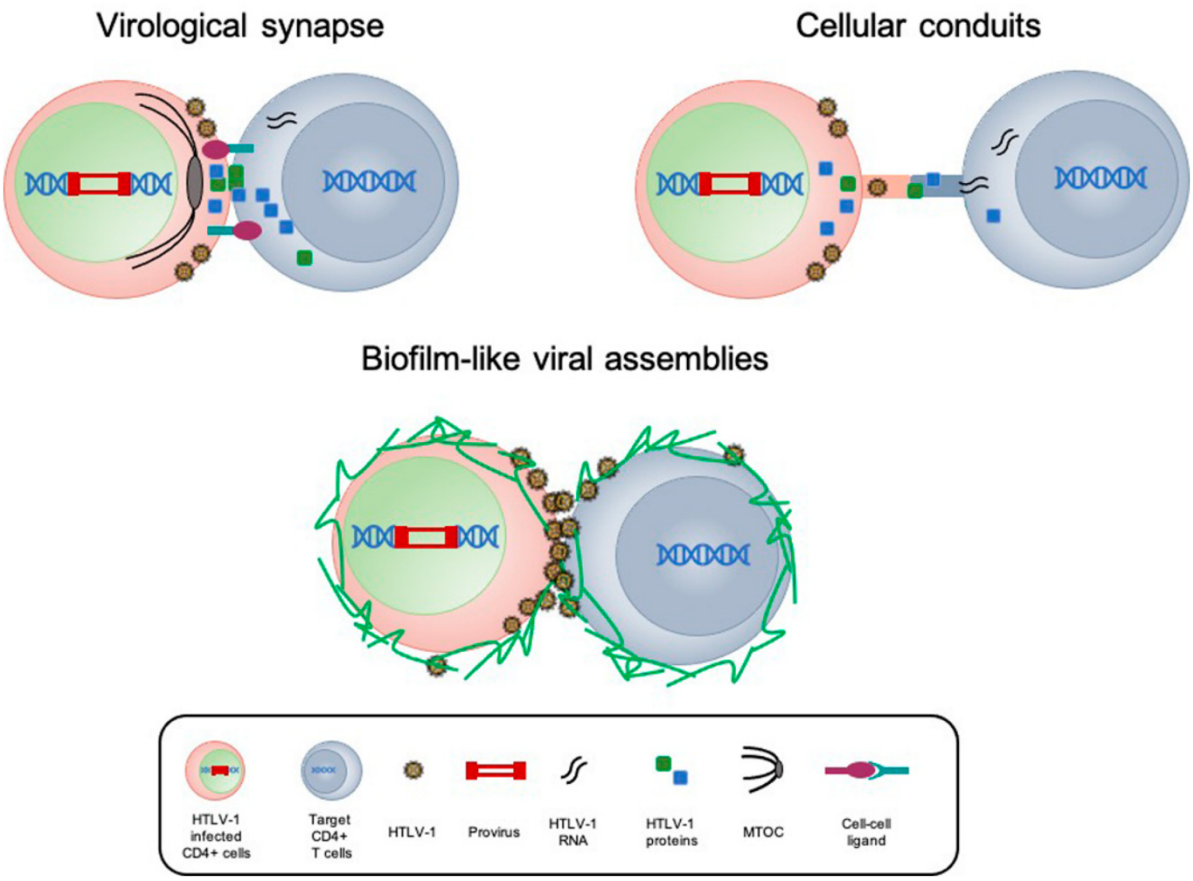

Figure 4: Models of HTLV-1 cell to cell transmission mechanisms in vivo. Three different ways of infection: polarized virus budding through a virological synapse; biofilms transmission and cellular conduits[49].

6) Viral spread

a) Infectious cycle

HTLV-1 has a similar life cycle to other retroviruses[50]. The life cycle of HTLV-1 begins with the binding of viral proteins (gp21/gp46 envelope proteins) to cell membrane surface receptors and their fusion (**Figure 5A**). This fusion allows the HTLV-1 capsid core containing the viral genome and viral proteins to be released into the cytoplasm of the permissive target cell (**Figure 5B**)[51,52]. Once the HTLV-1 genetic material enters the cell, reverse transcription of the HTLV-1 viral RNA genome into double-stranded DNA (dsDNA) by the reverse transcriptase within the capsid occurs (**Figure 5C**)[52,53]. The resulting double-stranded viral DNA enters the nucleus (**Figure 5D**) and integrates into the host genome (**Figure 5E**), forming the provirus (**Figure 5F**). Subsequently, viral RNA is synthesized by the cellular machinery with the proviral DNA as a template (**Figure 5G**) and splicing of the transcripts to form viral mRNAs (**Figure 5I**)[52].

Rex accumulates in the nucleus and induces viral mRNA splicing. Singly spliced (env) and unspliced (gag-pro-pol) mRNAs are then exported from the nucleus to the cytoplasm leading to the production of viral proteins (**Figure 5J**)[52,53]. This is followed by the assembly (**Figure 5K**) and budding of virions[52]. The assembly of viral proteins leads to the formation of an immature virion which is then released from the cell by budding (**Figure 5L, M**)[52,54]. The budding virion then undergoes maturation via proteolytic treatment (viral protease), encoded by the Pro gene (**Figure 5N**)[52]. The viral protease cleaves the Gag and Pol polyproteins to produce a mature virus particle, ready to infect new cells[52,53].

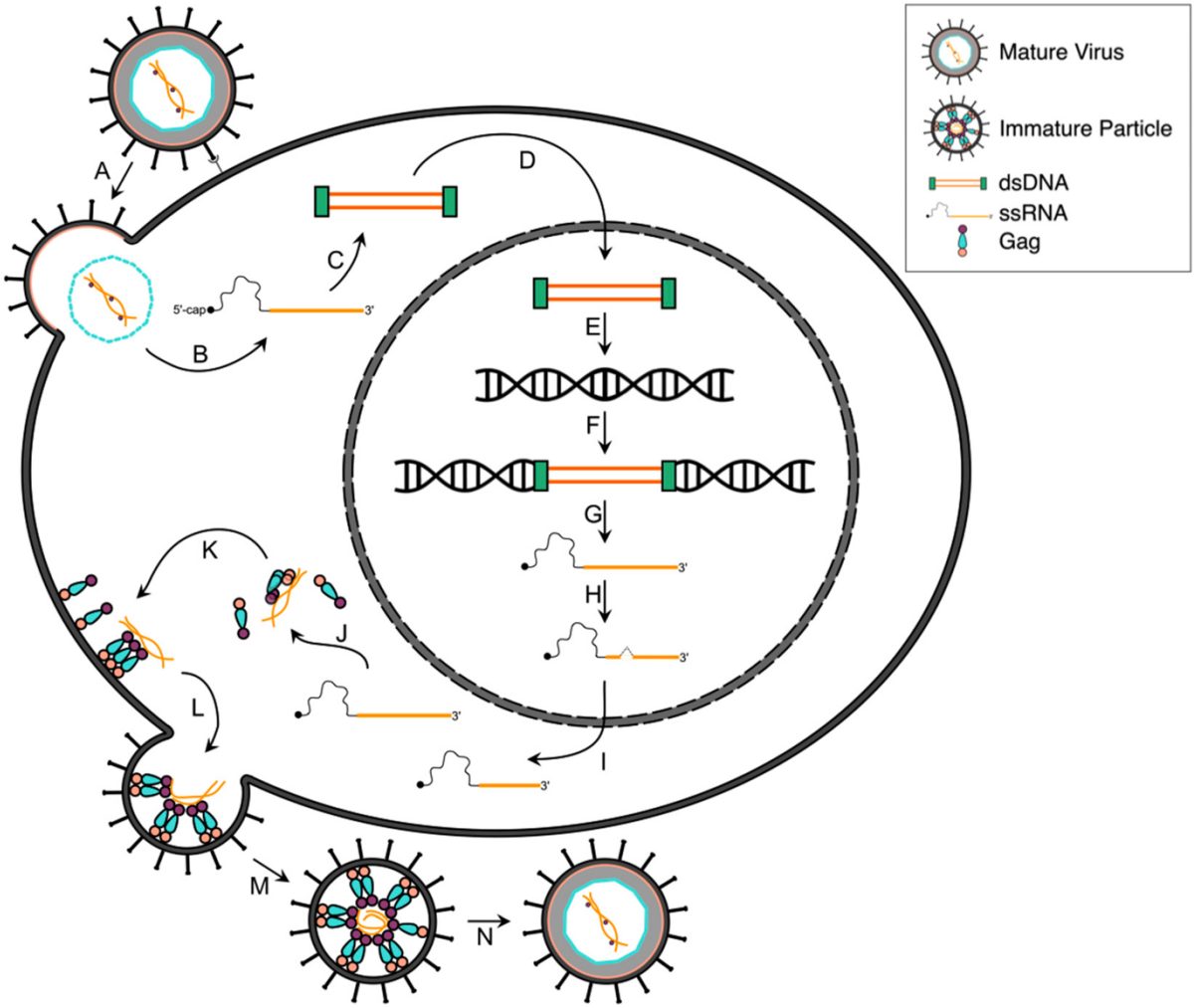

*Figure 5: HTLV-1 infectious life cycle. The virus interacts with viral envelope proteins with HTLV receptors and viral particle fusion with cell membrane **(A)**. Uncoating of viral core **(B)** and reverse transcription of viral positive strand RNA into DNA **(C)**. Entry of viral DNA in the nucleus **(D)** and integration of proviral DNA into host cellular DNA **(E, F)**. Following integration, provirus transcription and splicing for formation of mRNAs **(G, H)**. Unspliced and partially spliced viral mRNAs are then exported from the nucleus to the cytoplasm by Rex **(I)**. Translation of viral proteins **(J)** and transport to the plasma membrane **(K)**. Virions assembly **(L)** and budding of immature virions from the cellular membrane **(M)**. Maturation of viral particle **(N)***[53]

b) Modes of propagation of HTLV-1 virus

After primary infection with HTLV-1, some viral proteins such as Tax promote the proliferation of infected cells and inhibit cell apoptosis by their pleiotropic effects[55]. Since the provirus integrates randomly into the host genome, it is possible to identify each infected clone and to follow the dynamics of infected cells in vivo by identifying the site of integration[56]. Since HTLV-1 infection occurred exclusively by cell-to-cell contact, the number of infected cells in vivo has a significant impact on viral spread. There are two modes of propagation of HTLV-1 virus in vivo after primary infection: propagation by cell-cell contact (*de novo infection*) and propagation by cell proliferation (clonal expansion) (**Figure 6**)[57,58].

During de novo infection, each newly infected cell has a unique integration site of the provirus leading to an increase in the variety of HTLV-1 infected clones [57]. During this *de novo infection*, Tax, is required for efficient viral replication[57]. Since Tax is highly immunogenic, *de novo infection* causes activation of the immune system against HTLV-1[57]. Clonal expansion increases the abundance of each clone as it is a proliferation of infected cells[57]. HBZ and Tax seem to play an important role in this clonal expansion because they promote the proliferation of CD4+ T-cells and then lead to the appearance of ATL after a long latency period[56,55,57]. Indeed, studies have shown that Tax and HBZ oncoproteins often act in opposite directions to control the host immune response and maintain long-term malignant transformation[59,60]. Therefore, due to the activation of the immune system during *de novo infection*, clonal expansion seems to be the main mode of propagation or viral persistence during the long-term carrier state and is responsible for maintaining a high proviral load [57,49].

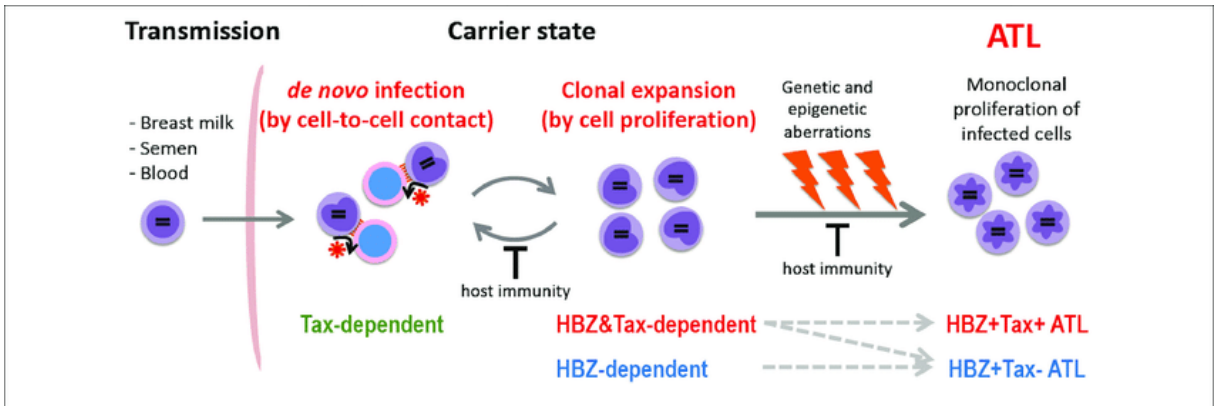

Figure 6: De novo infection and clonal expansion[57]

7) HTLV-1 oncoviral proteins

HTLV-1 encodes several proteins but two proteins play an important role in oncogenesis: Tax and the basic leucine zipper (HBZ) of HTLV-1. Together, these two proteins contribute to the survival of HTLV-1infected cells[61] and promote T cell proliferation.
Studies in Tax/HBZ double transgenic mice show that Tax and HBZ synergistically dysregulate cell signalling pathways in ATL and determine cell fate. These two oncoproteins are sufficient for the development of ATL in the absence of any other viral gene[53,62]. Importantly, these two oncoproteins have distinct functions in the genesis, regulation of cell activity and maintenance of ATL[53,61,62].

a) Tax oncoprotein

The multipotent HTLV-1 Tax oncoprotein is found primarily in the nucleus but is also found in the cytoplasm based on cell fractionation and light microscopy studies[63,64].
Tax has a molecular weight of 40kDa[65], is encoded from a spliced mRNA. Tax is a transcriptional transactivator and a central player in the regulation of viral gene expression, viral replication and proliferation of HTLV-1 infected cells[56]. Able to complex with more than 100 cellular proteins of different functional groups, Tax up or down-regulates several cellular genes[66,67]. Therefore, it also interferes with the ability of several cellular signal transduction pathways as well as the activity of many cellular effectors[63]. Studies have shown that Tax interacts with family of transcription factors such as cyclic AMP response element binding protein/activating transcription factor (ATF/CREB), NF-κB and serum response factor p67 (SRF) [56,63,67]. The interaction of Tax with ATF/CREB leads to increased dimerization and ATF/CREB binding affinity to Tax-responsive elements (TRE) found in the 5' long terminal repeat (LTR) of HTLV-1[63,68]. Tax is considered the primary T-cell activation effector as it transforms human T-cells leading to the development of T-cell leukemia in adults[56,63]. It is important to note that Tax is not expressed in 60% of ATL cases due to accumulation of genetic alterations (deletions), epigenetic modifications (hypermethylation) of the 5'LTR, as well as genetic modifications of the Tax sequence[69, 63,70,71]. Other activities are also attributed to Tax such as the perturbation of cell cycle progression by acting on cell regulatory effectors involved in the passage through cell cycle checkpoints[63,72]. Tax also affects mechanisms involved in the DNA damage response and apoptosis pathways and it activates the expression of specific cellular genes involved in T-cell proliferation and differentiation via activation of the NF-κB pathway[69,66,72]. Regarding its structure (**Figure 7**), we find at the N-terminal end (amino acids 18 to 52), a Nuclear Localization Signal (NLS) that covers an interaction domain with Zn

located at amino acids 23 to 62[63]. In the central Tax domain (from amino acid 188 to 202), there is a nuclear export signal (NES) coinciding with a leucine-rich sequence (LR)[63,73]. It is important to note that several domains are involved in Tax functions. At the N-terminal end, there are domains for the interaction of Tax with CREB and with the transcriptional coactivators CBP and p300 as well as a domain for the contact of Tax with DNA[63,74]. At the C-terminal end, the domains important for transcriptional activation (amino acids 289-322) and for the interaction of Tax with CBP and p/CAF are present[63,75].The formation of the Tax/CREB/CBP/TRE quaternary complex involved in the activation of the HTLV-1 promoter by Tax via the ATF/CREB pathway is regulated by these N- and C-terminal domains[63,76]. Domains for activation of cellular gene expression via the NF-κB pathway and sites for Tax interaction with IKK/NEMO or transcriptional coactivator p300 are in the central region of the Tax oncoprotein (**Figure 7**)[63,77,78]. The PDZ binding domain marks the end of the Tax carboxy end[63].

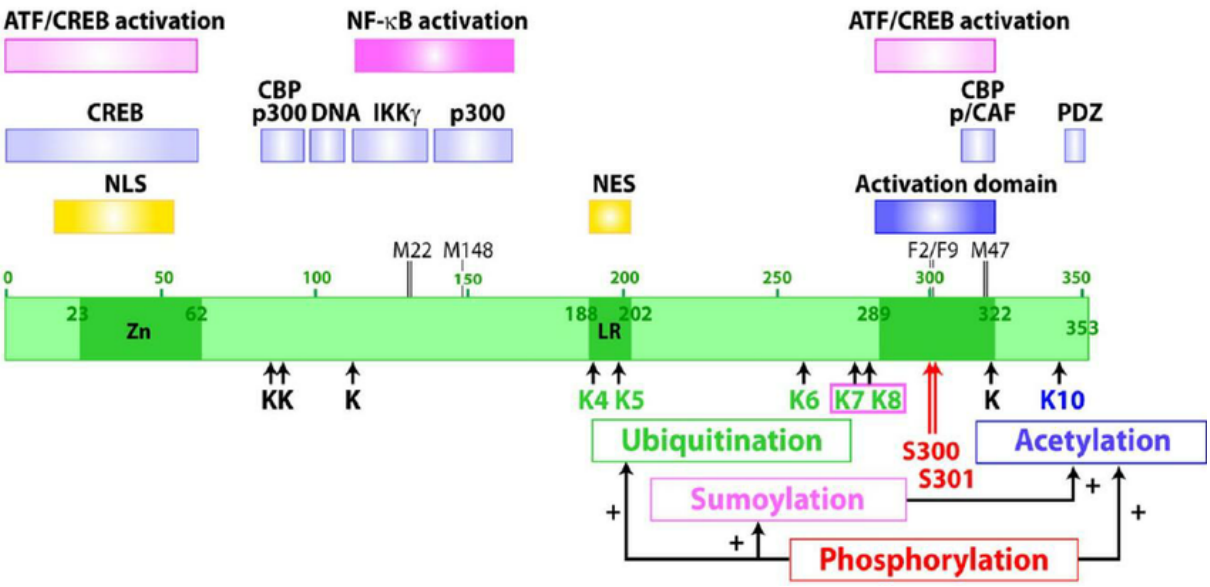

Figure 7: Map of HTLV-1 Tax oncoprotein structure[63].

b) HBZ oncoprotein

As mentioned above, the pX region of the HTLV-1 genome encodes the accessory gene HTLV-1 basic leucine zipper factor (HBZ) by alternative mRNA splicing. It is important to note that only HBZ is encoded on the antisense strand of the provirus[79]. It has been shown that HBZ is expressed and retained in all cases of ATL concluding the indispensability of this oncoprotein for HTLV-1 infection and ATL development[69]. It appears that HBZ mRNA plays a different role in T-cell proliferation than HBZ oncoprotein[53]. HBZ plays an important role in the dysregulation of several cellular processes in concert with Tax, affecting cell proliferation, apoptosis, autophagy and immune evasion[70].

8) HLTF

Predominant in the nucleus, the helicase-like transcription factor (HLTF) is a protein belonging to the SWItch/Sucrose Non-Fermenting (SWI/SNF) protein family[80]. HLTF is the human homolog of the RAD5 (S. cerevisiae).

a) Structure of HLTF

Located on chromosome 3q25.1-q26.1, the human HLTF gene is 56.4Kb long with 22-26 exons[80]. In most human tissues, two HLTF mRNAs of 5.5 and 4.5kb are expressed[80]. These RNAs differ in the alternative splicing undergone in the 3' untranslated region (UTR). Since these two mRNAs contain two translation start sites in the same reading frame (Met1 and Met123 codons), this leads to the synthesis of two protein forms with distinct amino termini[80]. The HLTF protein has a molecular weight of 110-115KD[81]. It is important to mention that the protein family (SWI/SNF) has 7 DNA helicase domains that use energy from ATP hydrolysis to remodel chromatin in various cellular processes[80,81].

Regarding the structure of HLTF, we find at the N-terminal end the HIRAN domain (HIP116 Rad5p) integrated in a larger DNA binding domain (DBD)[82]. Then we find at the N-terminal end, a dimerization domain called Sucrose Non-Fermenting 2 (SNF2). Then the 7 conserved DNA helicase/ATPase domains characteristic of the SWI/SNF2 family. And finally, the RING finger domain characteristic of E3 ubiquitin ligases separates the N and C terminal end of the SWI/SNF helicase domain (**Figure 8A**)[80,82].

Alternative splicing of HLTF pre-mRNA in the region of exons 19-20 generates two reading frame shifts resulting in truncated protein forms: one with a deletion of the RING finger (HLTF Met1ΔA (83 kDa)) (**Figure 8B**) and the other with the loss of the last 3 DNA helicase domains using energy from ATP hydrolysis specific to the SWI/SNF family (Met1ΔB (95 kD)) (**Figure 8C**)[80,81].

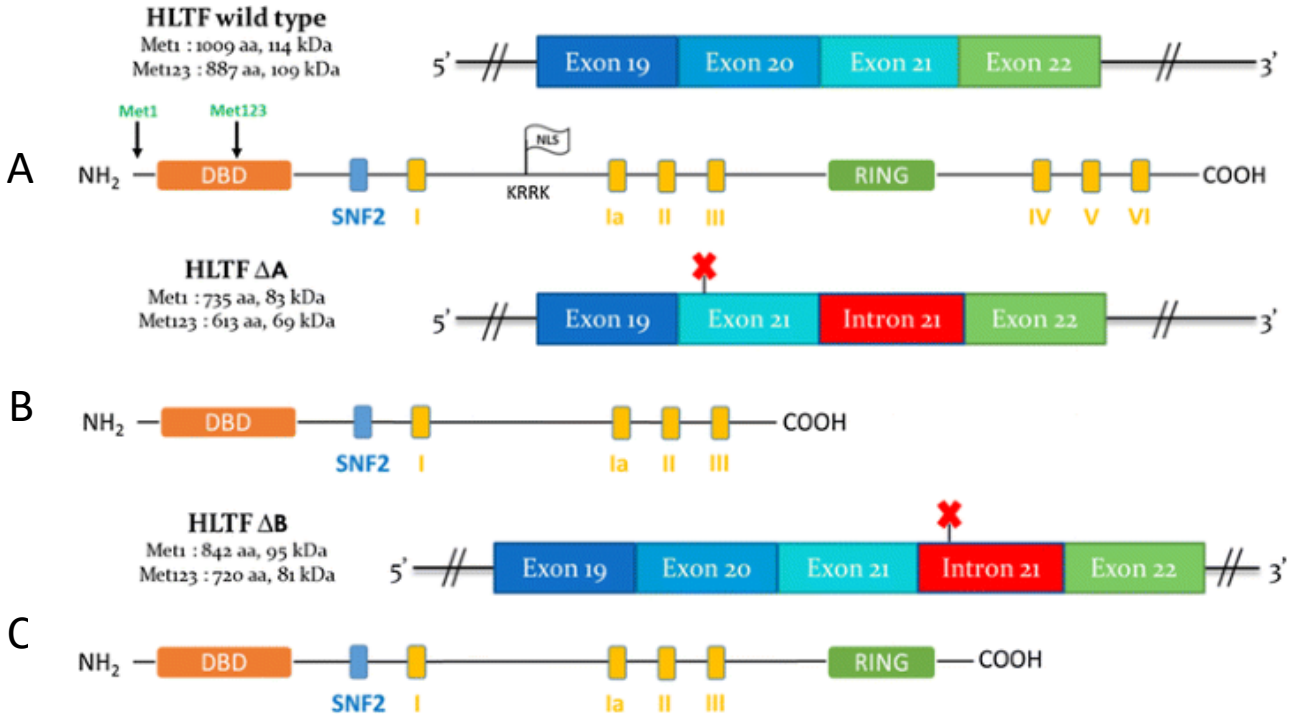

Figure 8: Alternative splicing and encoded proteins of HLTF[80].

b) Cellular function of HLTF

HLTF is involved in gene transcription, DNA repair, and maintenance of genome stability (role in tumor suppression)[80].

i) Transcription factor

HLTF is a highly conserved protein across species. Due to its ability to bind specifically to DNA sequences and modulate transcription by modifying chromatin structure, HLTF has been identified as a transcription factor. HLTF is, therefore, able to recognize replication fork-like structures associated with its interaction with DNA sequences[80]. HLTF induces the expression of genes involved in various pathways (DNA repair, apoptosis, cardiac development and cell

cycle: G2-M transition)[80]. Studies have shown that HLTF is important for the maintenance of genomic stability because its loss increases the frequency of chromosomal abnormalities in case of DNA damage[82].

ii) Post-replication DNA repair

Since DNA is constantly subject to endogenous and exogenous events that cause damage, DNA repair processes aim at eliminating lesions to avoid aberrant DNA replication. Indeed, aberrant DNA replication is the cause of mutations, double-strand breaks, and chromosomal rearrangements associated with pathological disorders[80,83].
HLTF is required to repair DNA damaged during replication, which supports its role as a tumor suppressor[80].

iii) Tumor suppressor

Indeed, HLTF expression is reduced in tumorigenic cells and thus in many cancers such as colon, esophageal and stomach cancer[80,84,85]. *Hibi et al* examined the methylation of HLTF in colorectal, gastric, and esophageal carcinomas. They demonstrated that HLTF could play various roles depending on the cell type[84]. Indeed, their experiments show that the HLTF gene was frequently methylated in colon and gastrointestinal cancers but not in oesophageal squamous cell cancer[84,85].
These results are concordant with studies indicating that HLTF expression is altered by one of two mechanisms: silencing by promoter hypermethylation or alternative splicing of the HLTF gene leading to truncated proteins lacking functional domains (involved in DNA repair)[80,84].

iv) Restriction factor

Restriction factors are natural antiviral proteins that limit viral replication and HLTF has been identified as such in a few diseases caused by viruses such as HIV, human cytomegalovirus[86], and other types of herpes viruses[87]. The HIRAN domain mediates the restriction of viral replication by HLTF[86]. The mechanisms by which HLTF performs its role as a restriction factor are still poorly known and understood. However, studies with the HIV virus show that there is

a relationship between antiviral activity and the ability of HLTF to modulate DNA damage repair.

9) NF-κB pathway activation

a) Structure of NF-κB

Nuclear factor kappa-light-chain-enhancer of activated B cells (NF-κB) is a protein complex that was first described in B cells in 1986 as a factor capable of binding to the immunoglobulin Kappa light chain gene enhancer[88]. Subsequent studies have shown that it is a ubiquitous transcription factor in all human cell types, playing a key role in proliferation, apoptosis, oncogenesis and immune response[89].

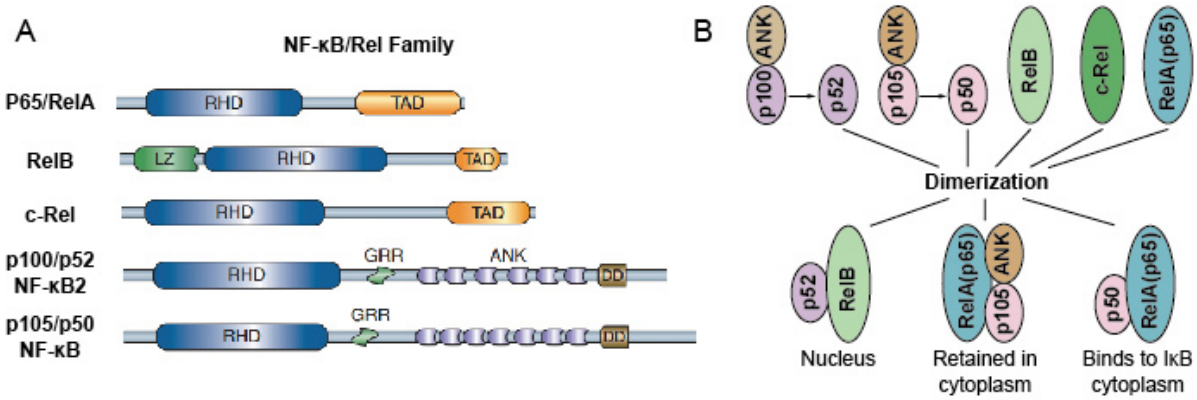

Figure 9: A) NF-κB family members B) Homo and heterodimeric of NF-κB family[90].

In mammalian cells, the NF-κB family of transcription factors includes five distinct protein members described so far: NF-κB 1 (p50 and pl05), NF-κB2 (p52 and p100), RelA (p65), RelB and c-Rel (**Figure 9A**)[88,91,92]. Each of these 5 proteins possesses the ability to form homo- and heterodimers[93] in all possible combinations except for the RelB protein, which dimerizes only with p50 or p52 (**Figure 9B**)[94]. Expressed in most cells, p50/RelA is one of the widely studied NF-κB dimers[91,92,94,95]. These five protein members share a common conserved N-terminal region of 300 amino acids called the Rel homology domain (RHD)[88,91,90]. This Rel homology domain (RHD) is essential and contains a dimerization domain, a DNA-binding domain (DBD), a region of interaction with the inhibitory proteins IκB[92] and the Nuclear Localization Signal (NLS)[65,94,90,96].

The protein members RelA (p65), RelB and c-Rel have a transcription activation domain (TAD) in their carboxyl-terminal region necessary for gene expression, and are absent from the p105

and p100 proteins, whose proteolysis results in the p50 and p52 proteins, respectively[91,92,96,97]. Therefore, the p50 and p52 proteins are unable to activate gene expression unless they associate with one of the TAD-containing NF-κB family proteins or recruit a specific coactivator[65,97]. Nevertheless, p50 and p52 could occupy DNA binding sites even without initiation of transcription. These two homodimer proteins thus act as transcriptional repressors[96]. In addition to these two transcriptional repressors, there is a third form of repression due to IκB proteins[96]. IκB proteins are inhibitory proteins of the ability of NF-κB to translocate and activate transcription factors[88]. Seven IκB family members have been identified and can be organized into: classical IκB (IκB-α, IκB-β, and IκB-δ), nuclear IκB (IκB-γ, Bcl3), and the NF-κB precursors (p100 and p105) (**Figure 10**)[88,94].

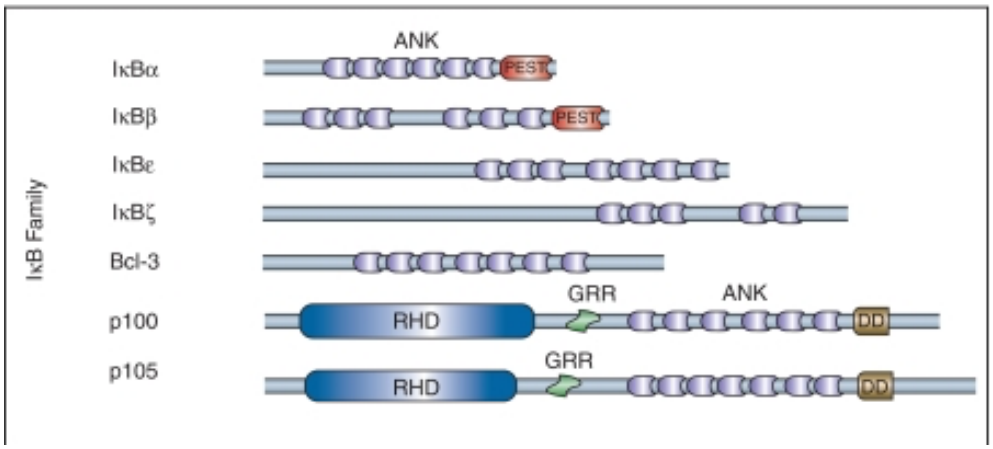

Figure 10: IκB family members and their structure.The domain indicated in each protein are: ANK: Ankyrin repeat, PEST: , proline-, glutamic acid-, serine-, and threonine-rich region, GRR: Glycin-Rich-Region,DD: Death Domain, RHD: Rel Homology Domain. [94]

These seven IκB proteins share a repeated ankyrin motif (30-33 amino acids), responsible for interacting with NF-κB[98] as a central domain functioning by binding to RHD[65,88,94]. This interaction masks the NLS (Nuclear Localization Signal) of the NF-κB proteins leading to the sequestration of the NF-κB family in the cytoplasm, which is unable to migrate into the nucleus and thus unable to induce gene transcription[94,96].

b) NF-κB function

NF-κB has several functions including the control of the immune response (innate and adaptive immunity) associated with inflammation at different stages, proliferation, and cell death. Innate immunity is facilitated by macrophages, dendritic cells and other specific cell types, which recognize via molecular patterns associated with pathogens, bacteria and viruses[99]. As

mentioned previously, NF-κB is constitutively active in the cytoplasm of most cell types except when induced by a stimulus to migrate to the nucleus[100].

Indeed, when cells are stimulated by bacterial toxins (LPS, exotoxin B), viral products, pro-inflammatory cytokines (IL-1α, IL-1β and TNF-α), cell death stimuli (free radicals, UV light, γ-radiation)[88,101] rapid activation of NF-κB and its translocation into the nucleus occurs to promote gene expression by binding to kB sites[88,100]. Due to the regulation of NF-κB activity by these different stimuli, NF-κB proteins can therefore be considered as regulators of cellular homeostasis[92]. In general, activation of NF-κB signaling occurs through two main pathways: a classical (canonical) pathway and an alternative (non-canonical) pathway.

i) NF-κB activation: canonical pathway

Activation of the canonical pathway is initiated when stimuli (bacterial toxins, pro-inflammatory cytokines...) bind to TNF receptors. RelA/p50 heterodimers are sequestered in the cytoplasm as inactive complexes by IκB inhibitory proteins[12].

This activates the IκB kinase complex (IKK) (composed of IKKβ, IKKα and NEMO (IKKγ) subunits[89,90,96]. The canonical pathway is NEMO-dependent for NF-κB activation.

This IKK complex then phosphorylates the IκB proteins which results in its ubiquitination as well as its degradation by the 26S proteosome [89,90,96]. The remaining active NF-κB /Rel complexes or NF-κB dimers (e.g., possibilities of p65/p50 or p50/p50 subunit combinations) are activated by post-translational modifications (phosphorylation, acetylation, glycosylation) and translocate to the nucleus, alone or in combination with other transcription factors (AP-1 Ets, and Stat)[91], (**Figure 11**). They then induce expression of the target gene (**Figure 11**)[90,102].

ii) NF-κB activation: non-canonical pathway

The non-canonical pathway is induced by specific members of the TNF (Tumor Necrosis Factor) cytokine family, such as BAFF (B-cell activating factor**)**, lymphotoxin-β, or CD40 ligand, which relies on IKKα, but not on IKKβ or IKKγ[89,94]. These signals are integrated by a NF-κB-inducing kinase (NIK) which activates the IKKα. The major distinction between the two signaling pathways lies in the dependence on NF-κB Essential Modulator (NEMO/IKKγ) and IKKβ[90]. Indeed, the non-canonical pathway is, therefore, IKKα-dependent and NEMO-independent unlike the classical (canonical) pathway[89].

IKKα then phosphorylates the p100 NF-κB subunit, which leads to proteosome processing of the p100 precursor to p52 (**Figure 11**)[89]. This results in the activation of transcriptionally competent p52-RelB heterodimers. The p52-RelB heterodimers translocate to the nucleus [90], alone or in combination with other transcription factors AP-1 (Activator Protein)[91], Ets, and Stat) and induce target gene expression (**Figure 11**)[102].

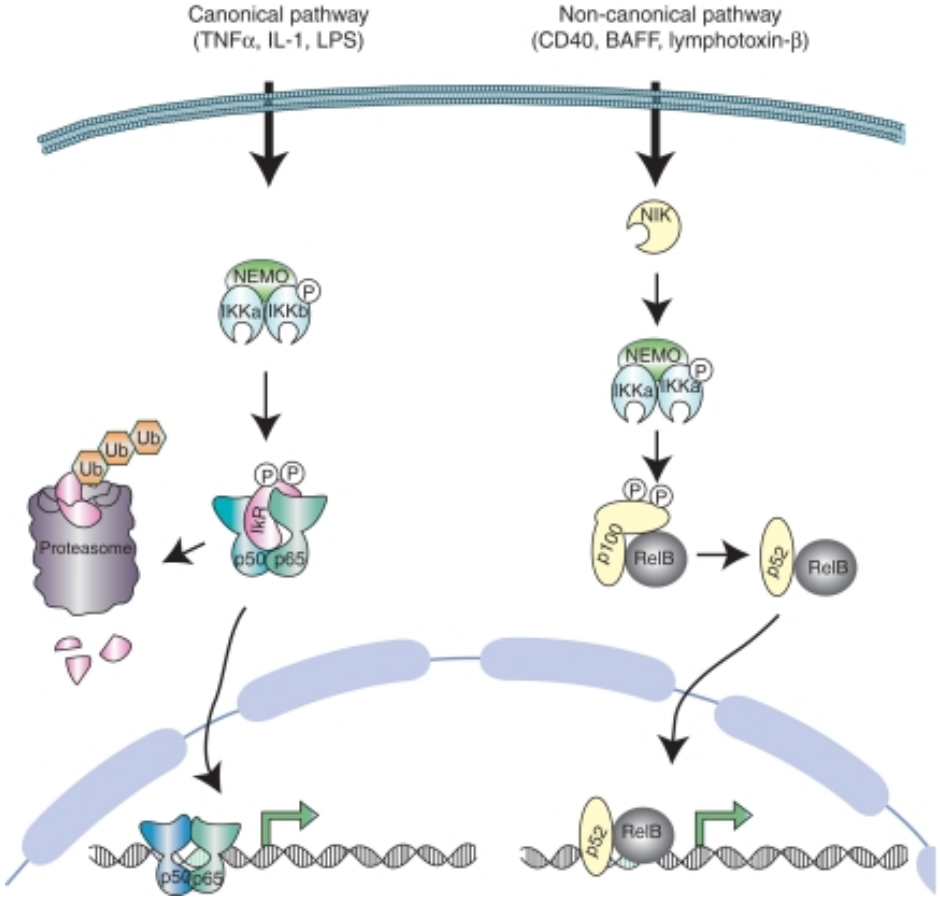

Figure 11: NF-κB signaling[94]

c) Tax-mediated NF-κB activation

The transcription factor NF-κB has been shown to participate in Tax-mediated transactivation and is involved in the regulation of many cellular genes [103,104]. The HTLV-1 Tax oncoprotein stimulates the constitutive nuclear expression of various NF-κB family proteins (p50, p52, RelA and c-Rel)[105,106] and interacts with various NF-κB and IκB family members[91,107]. When bound to p100, Tax is mainly cytoplasmic and is nucleated when bound to p52[108]. Interaction with the p105 and p100 precursors allows the active NF-κB family members to be retained in the cytoplasm[103]. Studies have shown that Tax interacts with the p105 precursor of the p50 subunit

of NF-κB , as well as with the p50 subunit itself, both in the presence and absence of a κB site[103].

The NF-κB signaling pathway is chronically activated in T-cells infected with HTLV-1 retrovirus. Tax thus induces nuclear translocation of NF-κB factor in various cell types[103,105] and acts at multiple levels to induce and maintain NF-κB activity[109]. Tax binds directly to the ankyrin motifs contained in these IκB proteins[109].

As an alternative to these proposed models, in HTLV-1 infected cells and in cells expressing Tax, the Tax oncoprotein can constitutively induce the canonical signaling pathway leading to phosphorylation and degradation of IκB and may also constitute the non-canonical signaling pathway[107,109]. Indeed, in the activation of the NF-κB pathway by Tax, phosphorylation, ubiquitination and the subsequent degradation of IκBa are essential[109,110]. Under normal conditions, NF-κB activation is transient and occurs most often through the canonical signaling pathway[109,].

i) Tax activation of the canonical NF-κB pathway

Three models of NF-κB activation mechanisms by the HTLV-1 oncoprotein Tax have been proposed: the dissociation model, the proteasome screening model, and the signal transduction model[105].

In the dissociation model, Tax interacts directly with the latent NF-κB/IκB complexes in the cytoplasm. This direct protein/protein interaction leads to the dissociation of the latent NF-κB/IκB complexes into the IκB-Tax and RelA/p50 complexes and then to the nuclear translocation of NF-κB (**Figure 12A**)[105]. In this model, there is no degradation by the proteasome. However, there is currently no convincing experimental evidence to support this model[107,105].

In the proteasome targeting model, Tax interacts with IκBa and p105 leading to NF-κB activation and disruption of NF-κB /IκB complexes[109]. Indeed, this model consists of IκB degradation and NF-κB release (RelA/p50) due to the anchoring of latent NF-κB/IκB protein complexes to the 26S proteosome by Tax (**Figure 12B**)[105].

In the signal transduction model, IκB of the latent NF-κB /IκB complexes is phosphorylated by activation of a cellular protein kinase by Tax. The phosphorylated form of IκB is subject to polyubiquitination as well as proteolytic degradation by the 26S proteasome resulting in nuclear translocation of NF-κB and activation of gene expression (**Figure 12C**)[91,105,111].

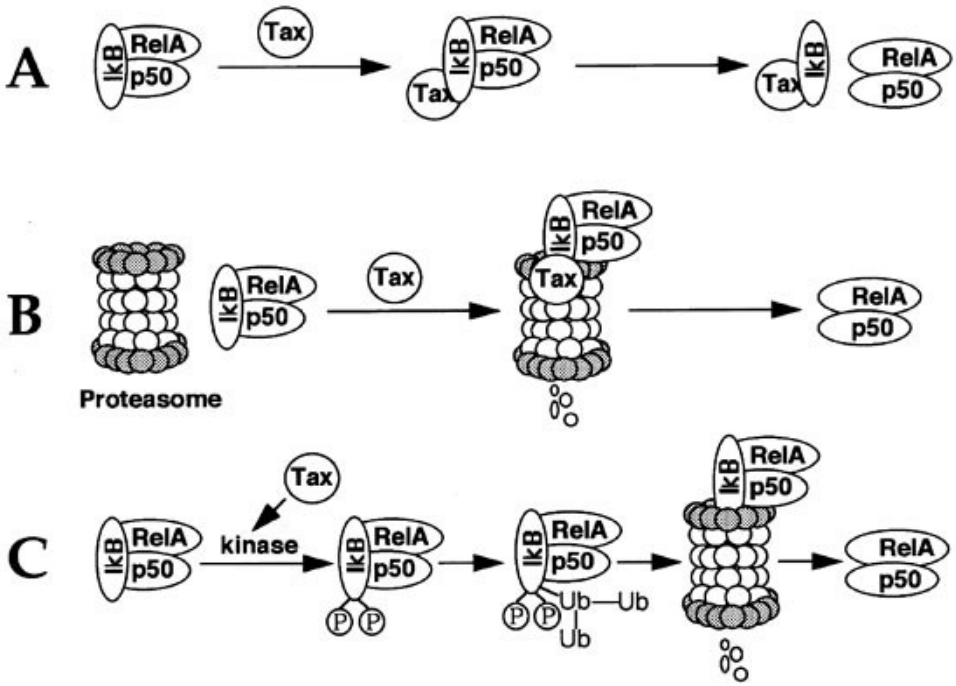

Figure 12: Models of NF-κB activation mechanisms by the HTLV-1 oncoprotein Tax A) Dissociation model B) Proteasome targeting model C) Signal transduction model[105].

Tax is a potent activator of nuclear accumulation of IκB and NF-κB.

Tax interacts with TAK1 (TGF-beta kinase 1) through the signal transducer Tab2, acting in this case as an adaptor molecule (**Figure 13**)[112]. Studies have shown that this interaction is essential to maintain constitutive activation of the IKK complex[112,113]. Tax then interacts with the regulatory subunit of the IKK-γ complex (NEMO) and stimulates the catalytic activity of IKK-α and IKK-β. Tax's interaction with TAK1 (TGF-beta kinase 1) and NEMO activates the IKK complex leading to phosphorylation, ubiquitination and degradation of IκB promoted by its interaction with proteasome[114]. This degradation of IκB exposes the NLS of NF-κB dimers (p50/RelA). Exposure of the NLS of the p50/RelA dimer leads to its rapid translocation to the nucleus and induces target gene expression (**Figure 13**)[109]. Tax-mediated canonical NF-κB signaling pathway requires both IKK-α and NEMO to activate NF-κB via the canonical route.

ii) Tax activation of the noncanonical NF-κB pathway

According to several reports of studies, no kinase activity has been attributed to Tax, therefore, to support the activation of the NF-κB pathway, Tax induces persistent phosphorylation and activity of the IKK complex[109]. Tax has been shown to bind to the IKK complex through TNF receptor-associated factor 3 (TREF3) (**Figure 13**). Indeed, Tax interacts directly with the

regulatory subunit of the IKK-γ complex (NEMO) mediated by the leucine zipper domains present in the C- and N-terminal portions of IKK-γ (NEMO) and the leucine repeat region (LRR) in Tax[105,109,115,116]. This direct interaction between Tax and IKK-γ (NEMO) allows the subsequent recruitment of the other catalytic subunits of the IKK complex (**Figure 13**)[109,116]. Cooperation of Tax with IKK allows physical recruitment of IKK-α to p100, triggering phosphorylation-dependent ubiquitination and transformation of p100 to p52[117] and also p100 degradation by proteasome. This degradation of p100 exposes the NLS of NF-κB dimers (p52/RelB). Exposure of the NLS of the p52/RelB dimer leads to its rapid translocation to the nucleus and induces target gene expression (**Figure 13**).

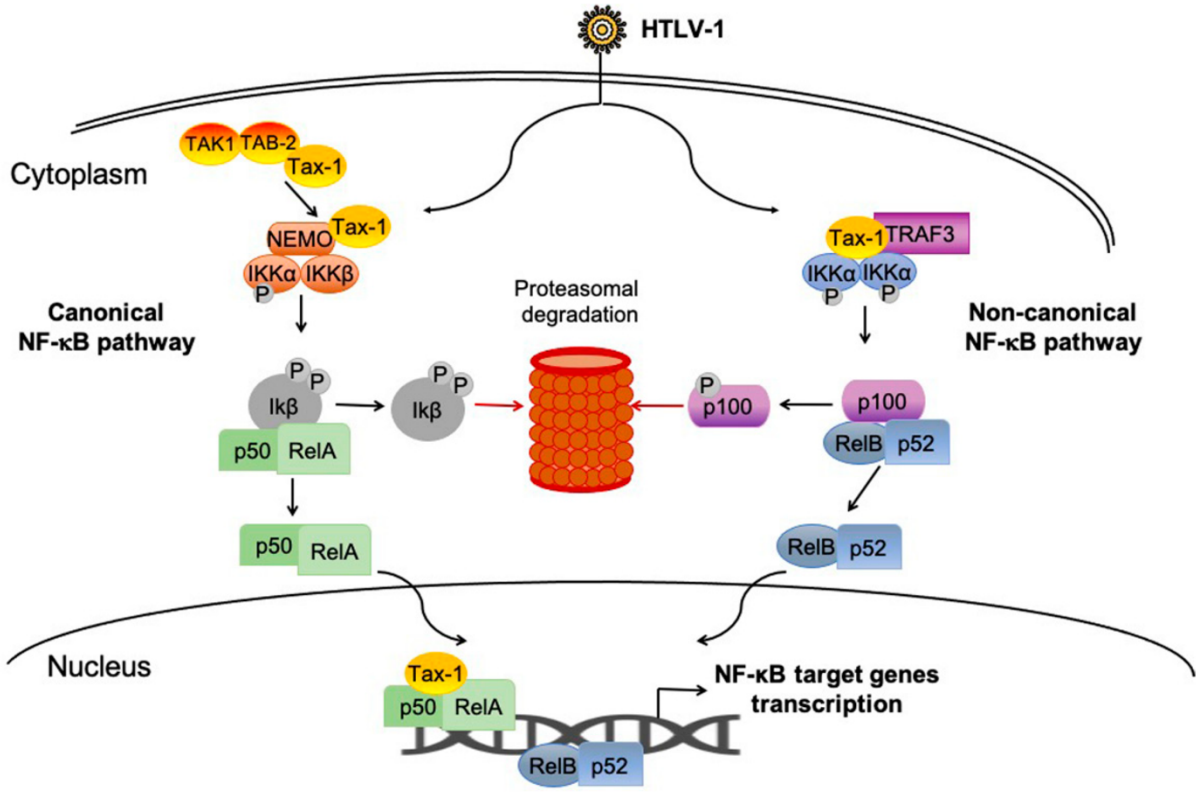

Figure 13: Mechanisms of Tax action on NF-κB activation[49].

In summary, Tax-mediated activation of the canonical and non-canonical NF-κB signaling pathway requires binding of Tax to NEMO and the IKK complex[12].

II) Objectives

The aim of this project is to evaluate the impact of Tax and HLTF on transcriptional activity directed by the HLTF promoter and the HTLV-1 long terminal repeat (LTR). Activation of the NF-κB pathway will also be assessed in presence of wild-type and mutants of HLTF and Tax.

The tasks will be to:

a) Verify the Tax and HLTF inductive system:

Expression of Tax and HLTF in HekiTax, HekiHLTF, HekiTaxiHLTF will be induced with doxycycline. The levels of Tax and HLTF expression will be analyzed by RT-qPCR and Western blot.

b) Evaluate the influence of Tax and HLTF mutants on the LTR promoter

To assess the effect of Tax mutants on LTR promoter activity, HekiHLTF cells transduced with a LTR luciferase reporter will be transfected with different Tax mutants. To evaluate the effect of HLTF mutants, cell lines expressing HLTF mutants (RING and HIRAN) in a doxycycline inducible system will be transduced with a LTR luciferase vector. Promoter activity will be evaluated by luciferase measurements after induction of HLTF expression.

c) Assess the influence of Tax and HLTF mutants on the HLTF promoter

To assess the effect of Tax mutants on the HLTF promoter, HekiHLTF cells cells transduced with a LTR luciferase reporter will be transfected with different Tax mutants. To evaluate the effect of HLTF mutants, cell lines expressing HLTF mutants (RING and HIRAN) in a doxycycline inducible system will be transduced with a HLTF luciferase vector. Promoter activity will be evaluated by luciferase measurements after induction of HLTF expression.

d) Evaluate the influence of Tax and HLTF mutants on the NF-κB activation pathway

To evaluate the influence of Tax mutants on the NF-κB pathway, HekiHLTF cells will be transduced with viral vectors expressing a nano-luciferase NF-κB plasmid. These transduced cells were then transfected with the Tax mutants.

The influence of HLTF mutants on NF-κB activity will be done in established cell lines expressing HLTF mutants (RING and HIRAN). These established cell lines will then be transfected with a nano-luciferase NF-κB plasmid.

NF-κB activity will be evaluated by luciferase measurements after induction of HLTF expression in the transfected cells with doxycycline.

III) Materials and methods

1) Cell culture

Established cell lines Hek293T (Hek, HekiTax, HekiTaxiHLTF, HekiHLTF, Hek_NF-κB, HekiTax_NF-κB, HekiTaxiHLTF_NF-κB, HekiHLTF_NF-κB, HekHLTF, HekMut_RING and HekMut_HIRAN) were grown in DMEM (1 g/l glucose, 2 mM glutamine) supplemented with 10% FBS, streptomycin at 100 µg/ml and penicillin at 100 U/ml. This DMEM solution is called complete DMEM. All cells were incubated at 37°C in a humidified 5% CO_2 atmosphere. Cells were thawed 1 week before the start of the experiment and maintained in culture up to 2 months. Cells were grown at density of 0.3-1.5 x 10^6 cells/ml and split every 3-4 days with appropriate antibiotics.

2) Plasmids digestion

Plasmids were digested for 1 hour at 37°C with the following enzymes: XbaI and EcoRI for Tax mutants and XbaI for HLTF mutants. Digested plasmids were then loaded on a 1% agarose gel and electrophoresis was carried out at room temperature for 45 minutes with a constant voltage of 100 Volts. Immediately after the run, the gel was revealed after exposition to ultra-violet (UV).

3) Transduction

a) Transduction with vector expressing NF-κB

NF-κB activation was quantified with the help of a lentivector containing NF-κB-dependent nano-luciferase gene (pLENTI6-AP-1-KB-NLUC-Pest-IRES-EGFP-V5). The lentiviral vector was produced by the GIGA Viral vector Platform. Briefly, Lenti-X 293T cells (Clontech) were co-transfected with gene transfert plasmid pSPAX2 (Addgene) and a VSV-G encoding vector. Viral supernatants were collected 48-, 72- and 96-hours post-transfection, DNAse treated, filtered (0.2µM) and concentrated 100-fold by ultracentrifugation. After suspension of the pellet in HBSS (Westburg #BE10-547F), the lentiviral vectors were titrated with the

qPCR Lentivirus Titration Kit (ABM, LV900). Lentiviral particles were transduced in Hek293T, Hek-iHLTF and Hek-iTaxiHLTF cells in 24 well-plates at 80% of confluence in complete DMEM containing 4µg/ml protamine sulfate. Luciferase activity was measured according to the Nano-Glo Dual-Luciferase Reporter Assay System (Promega) using a Tristars LB942 microplate reader.

b) Transduction of HLTF mutants

HEK293FT cells were seeded at a density of $2{,}5\times10^4$ cells/well in 6-well plates 1 day prior to transfection experiments and grown in complete DMEM. HEK293FT cells were transfected with a total of 3µg of DNA consisting of VSV-G, psPAX2, DNA of interest in a 1:2:4 ratio respectively. A mixture of 3:1 (w/w) PEI/DNA with 200µL of serum-free OPTIMEM was incubated for 15 min at room temperature and then added dropwise to the 6-well plates. The day before the transduction, cells to be transduced (Hek) were seeded at a density of 5×10^4 cells/well in 6-well plates. Twenty-four hours after seeding, the supernatant from transfected HEK293FT cells was collected in Eppendorf tubes. Polybrene (hexadimethrine bromide) was added to the supernatant at a final concentration of 3.33 µg/ml and mixed by pipetting up and down. The mixture was incubated for 15min at room temperature and then dispensed dropwise into the corresponding wells. Three days after transduction, cells were selected with the appropriate antibiotics. To produce the HLTF inducible system, Hek cells were first transduced with the TetON-3G transactivator, then with HLTF wild-type or HLTF mutants (Mut_RING or Mut_HIRAN) under the control of a TREG3G promoter (TREG3-hHLTF-His).

4) Transfection

Cells were seeded at a density of 1×10^4 cells/well in 24-well plates 1 day prior to transfection experiments and grown in the appropriate medium with 10% fetal bovine serum (complete DMEM). Polyethyleneimine (PEI)/plasmid DNA weight ratio 3/1 were used to prepare the polycation/plasmid complexes (i.e., polyplexes). The plasmid used for Tax mutants are pSG5, pSG5Tax, 2-28, 2-55, M22 (T130A/L131S), M47 (L319R/L320S), M148 (G148V), K88A, lysine-to-arginine Tax_His mutants (K1-3R, K1-10R, K6-8R, K4-10R) and HLTF mutants are HLTF wild type, Mut_RING, Mut_HIRAN. PEI/DNA mixture was added dropwise to the wells of 24-well plates. The yellow fluorescent protein (YFP) vector was used as a transfection

control. Twenty-four hours post-transfection, the medium was removed, and cells were induced with`1µg/mL of doxycycline in complete DMEM. Forty-eight hours after induction, the medium was removed, and the cells were washed with 500µL of PBS. Luciferase activity (LTR activity, HLTF-promotor activity and NF-κB activity for HLTF mutants) was measured using the Renilla Luciferase Assay kit (Promega). Briefly, cells were lysed with 90µL of passive lysis buffer (Promega), incubated for 15min on ice, then luciferase activity was measured using a Tristar s LB942 microplate reader. The Nano-luciferase activity (NF-κB activity for Tax mutants) was measured using the Promega Nano-Glo Dual-Luciferase Reporter Assay System kit (Promega): cells were lysed with 100 µL of trypsin, incubated for 5min at 37°C, then nano-luciferase activity was measured. The results are expressed as relative light units (RLU) of seeded cells.

5) RT-qPCR

Total RNA extraction from transfected cells was performed according to the manufacturer's protocol using the Nucleospin RNA Plus kit (Macherey Nagel). Then, using the reverse transcription kit (FastGene Scriptase II cDNA), cDNA was obtained by reverse transcription with random primers. The specific primers used were as follows: Tax gene: ACCAACACCATGGCCCA (fw), GAGTCGAGGGATAAGGAAC (rev), HLTF gene: GTTCAAAGATTAATGCGCT (fw), AAAGACAGGAATGTTGTAAACTGAGA (rev), HPRT gene: AAGGGCATATCCTACAACAAAC (fw), GGTCAGGCAGTATAATCCAAAG (rev). Transcripts of Tax and HLTF mutants were quantified by qPCR with Takyon No Rox SYBR 2X MasterMix (Eurogentec). qPCR was performed under the following conditions using the LightCycler 480 PCR: 2 min at 50°C, 3 min at 95°C, followed by 45 cycles of 10 seconds at 95°C and 45 seconds at 60°C. The ΔΔCt method was used to analyze the relative levels of target mRNA with HPRT as an internal control. A one-way ANOVA was performed to detect statistically significant differences between the means.

6) Western blot

Cells were lysed in RIPA buffer (50 mM Tris-HCl, pH 8, 150 mM NaCl, 1.0% NP-40, 0.5% sodium deoxycholate and 0.1% SDS) supplemented with protease inhibitors (Thermo Fisher)

on ice for 30 minutes. Lysed cells were then centrifuged at 14000rpm for 15min. Supernatants were collected, and protein concentration was determined using the Pierce BCA protein assay kit (Thermo Fisher), as well as a VICTOR X3 multi-label plate reader. The assayed proteins were then diluted in Laemmli 4X buffer (200mM Tris-HCl, pH 6.8, 8% SDS, 0.4% bromophenol blue, 40% glycerol) and denatured at 95°C for 5 minutes. Then, 50g of protein were loaded and separated by sodium dodecyl sulfate polyacrylamide gel electrophoresis. The gel was then transferred to a nitrocellulose membrane. Subsequently, these membranes were blocked for 45 min with 5% BSA-TBST (20mM Tris, 10mM NaCl, pH 7.5, 5% bovine serum albumin) at room temperature (RT). Membranes were then incubated overnight (O/N) at 4°C with anti-Tax (isolated from mouse), anti-HLTF (Sigma-Aldrich HPA015284) or anti-tubulin antibodies, followed by a one-hour incubation at RT with HRP-conjugated secondary antibodies (Dako anti-mouse P0260; Cell Signaling anti-rabbit 7074). Membranes were then visualized by chemiluminescence with ECL (ECL, Thermo Fisher) and protein bands were visualized with the ImageQuant LAS 4000 imager and quantified with ImageJ (NIH).

IV) Results

1) Characterization of established cell lines

Tax and HLTF expression of the established cell lines (HekiTax, HekiHLTF, and HekiTaxiHLTF) were induced with doxycycline (**Figure 14A**) for 48h. The inducible Tax and HLTF system was confirmed at the transcriptional level by RT-qPCR (**Figure 14B-C**) and at the protein level by western blot (**Figure 14D**).

Results indicate that Tax RNA levels increased significantly in the induced HekiTax (15-fold) and HekiTaxiHLTF (8.8-fold) cell lines compared to the uninduced cell lines ($p=0.0002$ and $p=0.0057$ respectively). Tax RNA levels were very low in the HekiHLTF cells (**Figure 14B**). HLTF RNA levels increased significantly in the induced HekiHLTF (9.5-fold) and HekiTaxiHLTF (11.5-fold) cells compared to the uninduced cell lines ($p=0.0003$ and $p<0.0001$ respectively). There was a very low level of HLTF RNA in the HekiTax cells (**Figure 14C**).

The western blot confirms this observation. Indeed, the protein level of Tax increases from 0 to 2.3 in HekiTax and to 1.7 in HekiTaxiHLTF after induction with doxycycline. The protein level of HLTF increases from 0.9 to 1.4 in HekiHLTF, and from 0.6 to 1 in HekiTaxiHLTF cells (**Figure 14D**). These results also show a reduction in HLTF expression after Tax induction.

Tubulin was used to normalize the protein levels detected because its amount is constant between cell lines. Tubulin, therefore, allows the quantification of Tax and HLTF proteins levels in the different established cell lines (**Figure 14D**).

In summary, these data demonstrate that Tax and HLTF are adequately expressed by the inducible system.

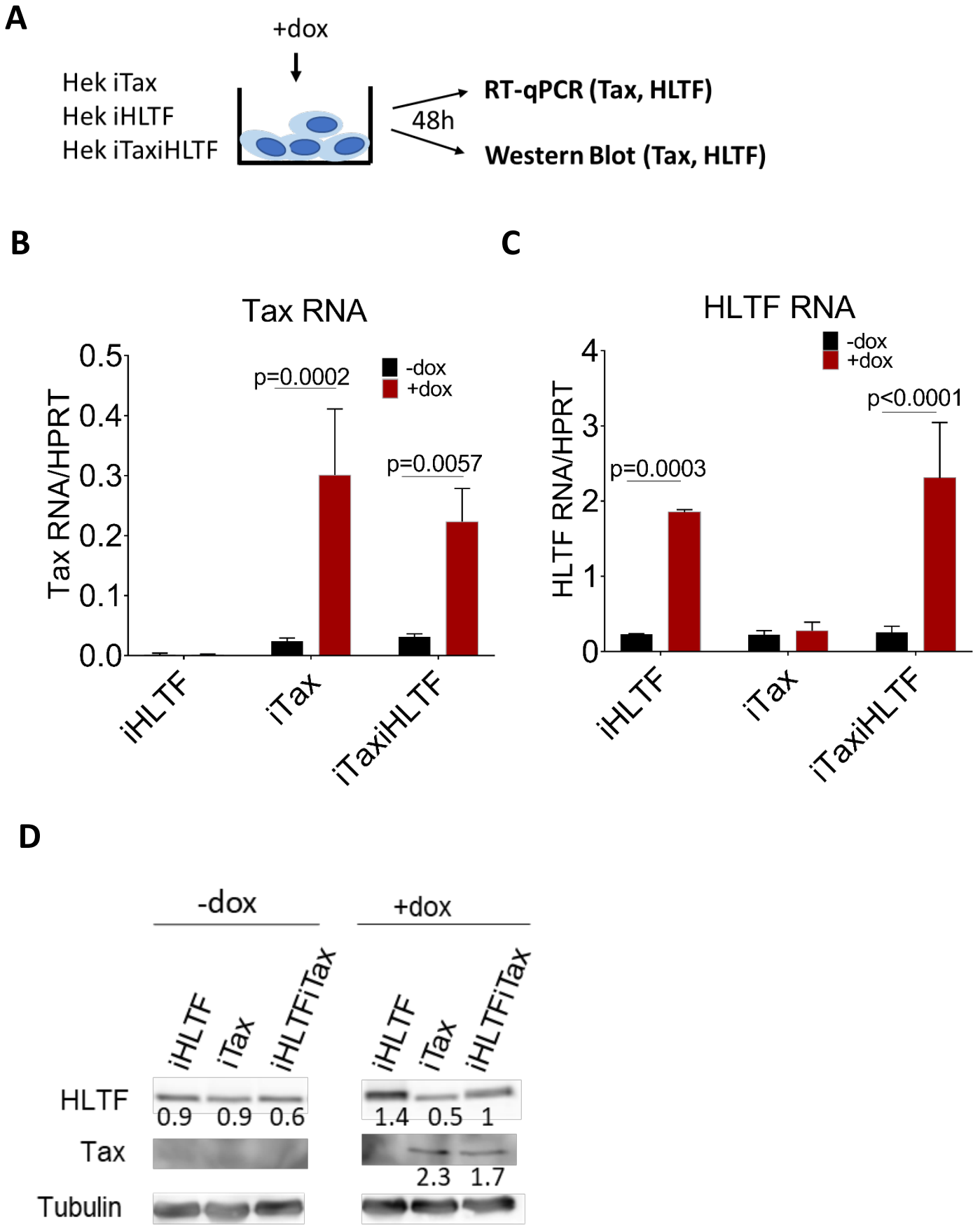

Figure 14: ***Characterization of established cell lines****. **(A)** Established cell lines (HekiTax, HekiHLTF, HekiTaxiHLTF) were induced with doxycycline and analyzed 48h later by RT-qPCR and Western-blotting. **(B-C)** Tax and HLTF transcripts were quantified by RT-qPCR. **(D)** Tax and HLTF protein levels were quantified by Western blotting**. The numbers below the bands represent the band intensities of Tax and HLTF levels normalized to tubulin levels. The statistical significance was determined by t test.*

2) Effects of established cell lines on NF-KB, LTR and HLTF promoter

The established cell lines (HekiTax, HekiHLTF, and HekiTaxiHLTF) were transduced with viral particles containing the NF-κB-AP-1-Luc plasmid (pLENTI6-AP-1-KB-NLUC-Pest-IRES-EGFP-V5). Transduced cells (HekiTax_NF-κB, HekiHLTF_NF-κB, HekiTaxiHLTF_NF-κB) were then incubated with doxycycline for 48h (**Figure 15A**). The NF-κB-AP-1-Luc plasmid was used to assess activation of the NF-κB pathway. Forty-eight hours after induction, luciferase activity was measured in relative luminescence units (RLU) with a luminometer (**Figure 15B**).

Results show that doxycycline-induced HekiHLTF_NF-κB cells do not express increased levels of luciferase, suggesting that NF-κB is not activated by HLTF. In induced HekiTax_NF-κB cellsthe luciferase activity increased by 20-fold compared to the uninduced cell lines ($p=0.001$), indicating that the NF-κB activity is stimulated by Tax. In presence of doxycycline, luciferase activity increased (22-fold) in HekiTaxiHLTF_NF-κB cells compared to the control ($p<0.0001$). In fact, luciferase activity was further stimulated in HekiTaxiHLTF_NF-κB cells compared to HekiTax_NF-κB cells (2.2-fold, $p=0.019$), suggesting a synergistic effect of Tax and HLTF on activation of NF-κB.

The cell lines (HekiTax, HekiHLTF, and HekiTaxiHLTF) were transfected with LTR-Luc or HLTF-Luc plasmids and induced with doxycycline for 48 hours (**Figure 15C**). The LTR-Luc and HLTF-Luc plasmids were used to assess transcriptional activation of the 5'LTR viral and HLTF promoters, respectively.

Forty-eight hours after induction, the luciferase activity was measured in relative luminescence units (RLU) (**Figure 15D-E**).

Analysis of LTR activity shows that induction of HLTF (HekiHLTF) has no influence on LTR activity (**Figure 15D**). Induction of Tax increases LTR activity (2.8-fold) as does simultaneous induction of Tax and HLTF (3.3-fold). However, the presence of HLTF neither reduces nor increases the transactivation activity of Tax on the LTR.

There is no influence on the HLTF promoter when both proteins (Tax and HLTF) are induced individually or simultaneously (**Figure 15E**).

In summary, the synergistic effect of Tax and HLTF on NF-κB-directed luciferase activity indicates that there may be an interaction between these two proteins in this pathway.

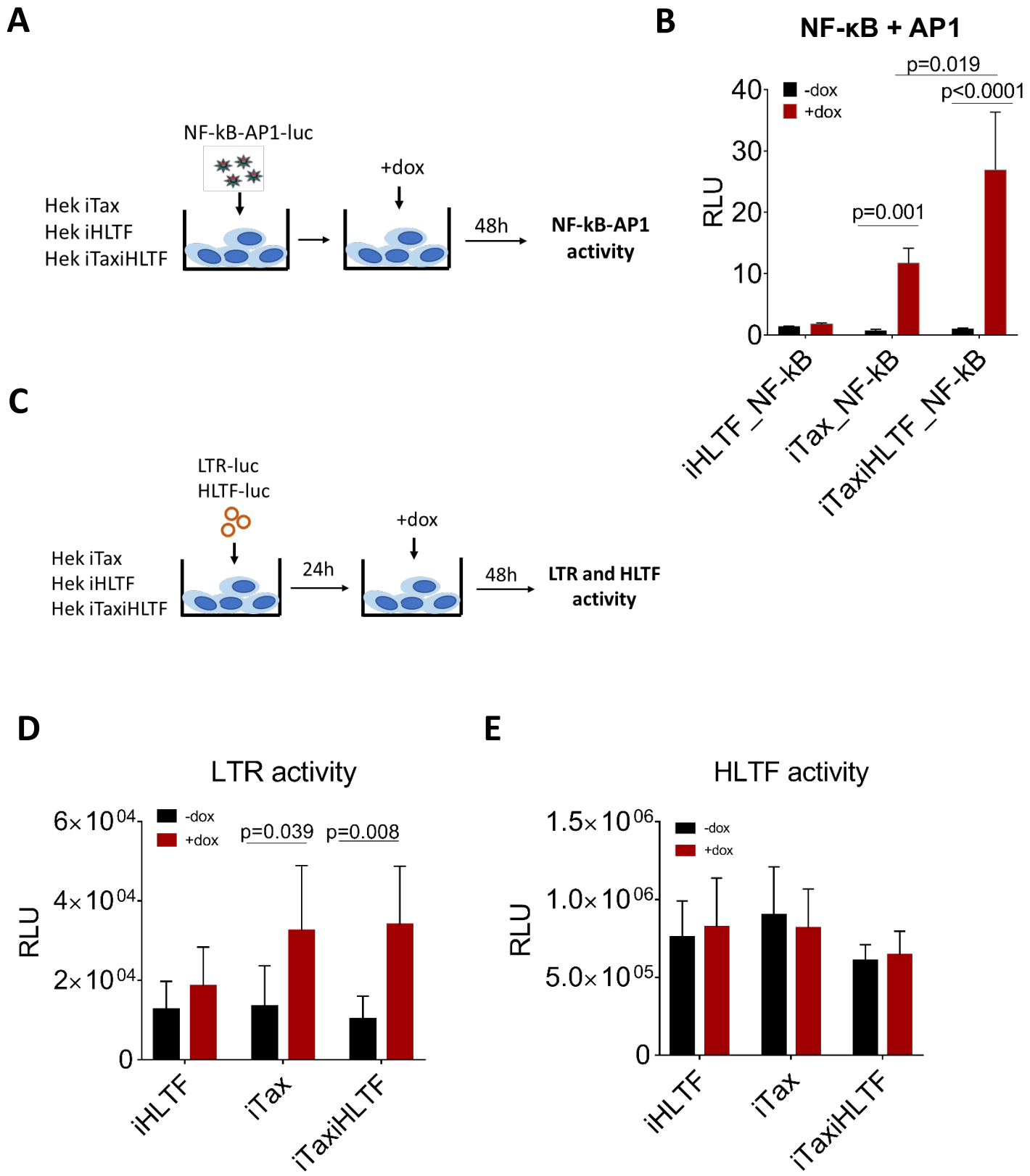

Figure 15: ***LTR and HLTF promoter activity and NF-κB activation in presence of Tax and HLTF****. **(A)** The established cell lines HekiTax, hekiHLTF, HekiTaxiHLTF were transduced with viral particles containing a NF-κB-AP1-Luc vector (HekiTax_NF-κB, HekiHLTF_NF-κB, HekiTaxiHLTF_NF-κB). The NF-κB activity was assessed by quantifying luciferase activity 48 hours after induction. **(B)** Luciferase activity was measured in relative luminescence units (RLU)**. (C)** The established cell lines HekiTax, HekiHLTF, HekiTaxiHLTF were transfected with the LTR-Luc or HLTF-Luc plasmids. The activity of the LTR and HLTF promoter was assessed by quantifying the luciferase activity 48 hours after induction**.** Luciferase activity was measured in relative luminescence units (RLU) **(D)** for LTR and **(E)** for the HLTF promoter. The statistical significance was determined by t test.*

3) Characterization of Tax and HLTF mutants

Plasmids containing the Tax and HLTF mutants were digested with the restriction enzymes XbaI and EcoRI and XbaI, respectively. The digested samples were loaded on a 1% agarose gel (**Figure 16A**). Results indicate that the fragments obtained after digestion correspond to the expected size, suggesting that the plasmids of the Tax and HLTF mutants used in the experiments are correct (**Figure 16C-D**).

Established HekiHLTF cell lines were transfected with the different Tax mutants: pSG5Tax, 2-28, 2-55, M22, M47, M148, K88A, lysine-to-arginine Tax_His mutants (TaxHis, K1-3R, K1-10R, K6-8R, K4-10R (**Figure 16**B) and analyzed by Western-blotting (**Figure 16E**).

Tax expression was detected by Western blot. The empty plasmid pSG5 was used as a negative control. The experiments show a constant amount of tubulin in each condition. Tubulin was used to normalize the intensity of the Tax and HLTF bands. Results of the western blot reveals the presence of HLTF protein in all samples. The amount of HLTF is lower in the lysine-to-arginine Tax_His mutants compared to Tax-His. Mutants 2-28, M47, K88A, K1-10R, K6-8R, K4-10R have a higher expression of HLTF compared to the negative control pSG5. The intensity of the Tax bands is lower for the 2-28 (0.35 intensity), 2-55 (0.28 intensity) mutants compared to Tax_WT (0.53 intensity) and for the lysine-to-arginine Tax_His mutants K1-3R (1.23 intensity), K1-10R (0.50 intensity), K6-8R (0.41 intensity), K4-10R (0.49 intensity) compared to Tax_His (1.87 intensity) (**Figure 16F**).

Hek cell lines were transduced with a doxycycline inducible system containing HLTF mutants (iHLTF, Mut_RING, Mut_HIRAN). Cells were then induced and Tax and HLTF protein levels were analyzed 48h later by western blotting (**Figure 16G**).

Tax expression was detected by western blot. Tubulin, used to normalize the intensity of the bands, is constant. The results show an increase in the amount of HLTF after induction with doxycycline: from 0.9 to 1.34 for iHLTF, from 0.75 to 1.45 for Mut_RING, and from 1.25 to 1.85 for Mut_HIRAN There is a higher amount in the induced HLTF mutants (Mut_RING, Mut_HIRAN) compared to the HLTF wild-type (iHLTF). The HIRAN mutant (Mut_HIRAN) has the highest amount of HLTF (**Figure 16H**).

Observation of the relative protein expression level of Tax and HLTF (Tax/HLTF) shows a ratio of 0.31 for 2-28, a ratio of 0.36 for 2-55, a ratio of 0.95 for M22, a ratio of 1.54 for M47, a ratio of 1.67 for M148 and a ratio of 1.51 for K88A to Tax_WT (1.18). For the Tax_His lysine-to-arginine mutants, there is a ratio of 1.30 for K1-3R, a ratio of 0.49 for K1-10R, a ratio of 0.29 for K6-8R and a ratio of 0.34 for K4-10R to Tax_His (1.08) (**Figure 16F**).

In summary, expression of a series of Tax and HLTF mutants was characterized. Mutants 2-28, 2-55 express the lowest amount of Tax compared to Tax_WT. Mutants 2-28, 2-55, K1-10R, K6-8R, K4-10R have a relative protein expression level of Tax and HLTF (Tax/HLTF) less than half that of Tax_WT or Tax_His respectively.

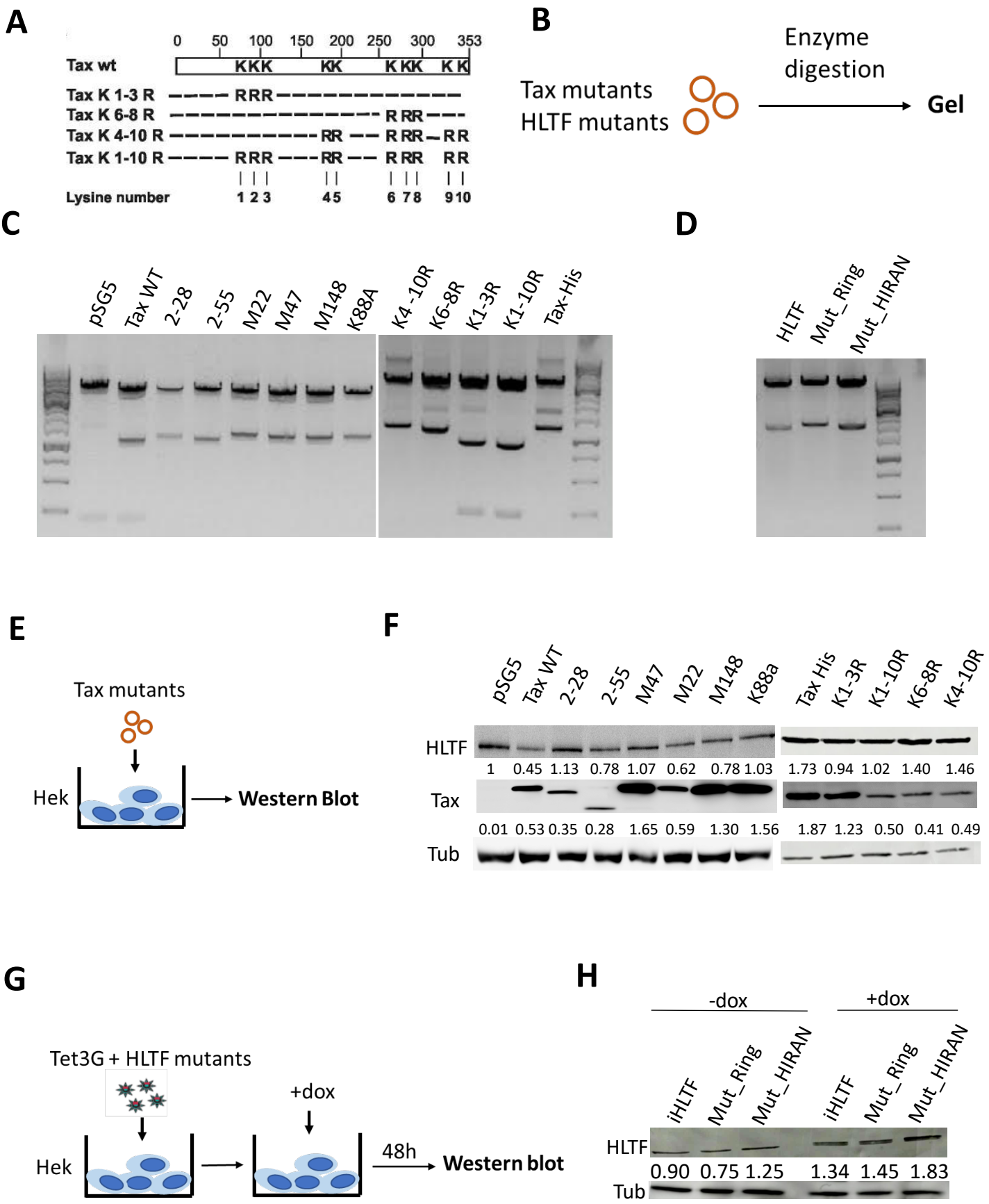

Figure 16: ***Characterization of Tax and HLTF mutants. (A)*** *Lysine-to-arginine Tax_ His mutants* ***(B)*** *Digestion of Tax and HLTF mutants. Tax mutants were digested with XbaI and EcoRI restriction enzymes and HLTF mutants were digested with XbaI restriction enzyme. Electrophoresis on 1% agarose was performed for* ***(C)*** *Tax mutants and* ***(D)*** *HLTF mutants.* ***(E)*** *Established Hek cell lines were transfected with the different Tax mutants (pSG5, pSG5Tax WT, 2-28, 2-55, M22, M47, M148, K88A, Tax His, K1-3R, K1-10R, K6-8R, K4-10R) and analyzed by Western-blotting.* ***(F)*** *Tax and HLTF protein levels were quantified by Western blotting.* ***(G)*** *Established Hek cell lines were transduced with a doxycycline inducible system expressing mutants of HLTF (HLTF_WT, Mut_RING, Mut_HIRAN). Transduced cells were then induced and HLTF expression was analyzed 48h later by Western blotting.* ***(H)*** *HLTF was quantified by Western blotting in the different HLTF mutants. The numbers below the bands in the western blot gel represent the intensities of the Tax and HLTF bands normalized to tubulin levels.*

4) Effects of Tax mutants

The established cell lines HekiHLTF were transfected with the different Tax mutants. LTR and HLTF promoter activities were analyzed 48h after induction of HLTF expression with doxycycline (**Figure 17A**).

The LTR activity curves were normalized to the plasmid Tax_WT signal or Tax_His signal whose activity was set to 100% (**Figure 17B**).

Some mutants such as 2-28, 2-55, M47, K88A and lysine-to-arginine Tax_His mutants such as K1-3R, K1-10R, K4-10R show very low LTR luciferase activity compared to Tax_WT or Tax_His. These mutants with low LTR luciferase activity are impaired for transcriptional activation of LTR excepting K1-3R.

Mutants defective in the LTR activation pathway compared to Tax-WT are 2-28 with a reduction of 82.5% ($p<0.01$), 2-55 with a reduction of 92.6% ($p<0.01$), M47 with a reduction of 77.8% ($p<0.01$), and K88A with a reduction of 85.2% ($p<0.01$). The lysine-to-arginine Tax_His mutants which do not activate the LTR are K1-10R with a reduction of 90.5% ($p<0.05$) and K4-10R with a reduction of 84.3% ($p<0.05$) compared to Tax_His. However, the K1-3R has a 71.4% reduction in luciferase activity compared to Tax_His, but this reduction is not significance.

Only M22 ($p=0.014$) and M148 ($p=0.043$) mutants shows a significant difference between induced and non-induced cells. Cells with HLTF induction show a decrease of Luciferase activity suggesting LTR activity reduction.

Mutants such as M22, M148, K6-8R induce transcriptional activation of LTR at levels comparable to the wild-type(Tax_WT or Tax_His for K6-8R) (**Figure 17B**).

Experiments to observe the effect of Tax mutants on HLTF promoter activation showed a similar pattern of curves. This would mean Tax mutants have no effect on HLTF promoter activation. It is important to note that these curves were not normalized with the Tax_WT plasmid (**Figure 17C**).

The established HekiHLTF_NF-κB cell lines were transfected with the different Tax mutants. NF-κB activity was assessed by quantifying the luciferase activity 48 hours after induction (**Figure 17D**).

Experiments to observe the effect of Tax mutants on the NF-κB activation pathway showed that 2-28, 2-55, M22, M148 mutants and lysine-to-arginine Tax_His mutants such as K1-10R, K6-

8R, K4-10R show a reduced NF-κB luciferase activity signal compared to Tax_WT or Tax_His respectively. These mutants are not all impaired for NF-κB transactivation. Mutants impaired (defective) for NF-κB transactivation compared to Tax-WT are 2-28 with a reduction of 84.7% ($p<0.05$), 2-55 with a reduction of 87.3% ($p<0.05$), M22 with a reduction of 83.4% ($p<0.05$), and M148 with a reduction of 58.5%. Although the reduction in NF-κB activity of the M148 mutant is lower than that of the other defective mutant, this reduction is not significant. The lysine-to-arginine Tax_His mutants which do not activate NF-κB activity are K1-10R with a reduction of 80%, K6-8R with a reduction of 80% and K4-10R with a reduction of 73% compared to Tax_His. A significant difference is observed between induced and non-induced cells for M47 ($p=0.013$), K88A ($p=0.002$), and K1-3R ($p<0.0001$).

However, some mutants, such as M47 and K88A induce NF-κB-sensitive transactivation at levels comparable to those of Tax_WT. The K1-3R mutant induces κB-sensitive transactivation at higher levels than Tax_His about 41.2%. NF-κB activity curves were normalized with the Tax_WT signal (**Figure 17E**).

Mutants 2-28, 2-55, K1-10R, and K4-10R are defective for the LTR transactivation and NF-κB activation pathway.

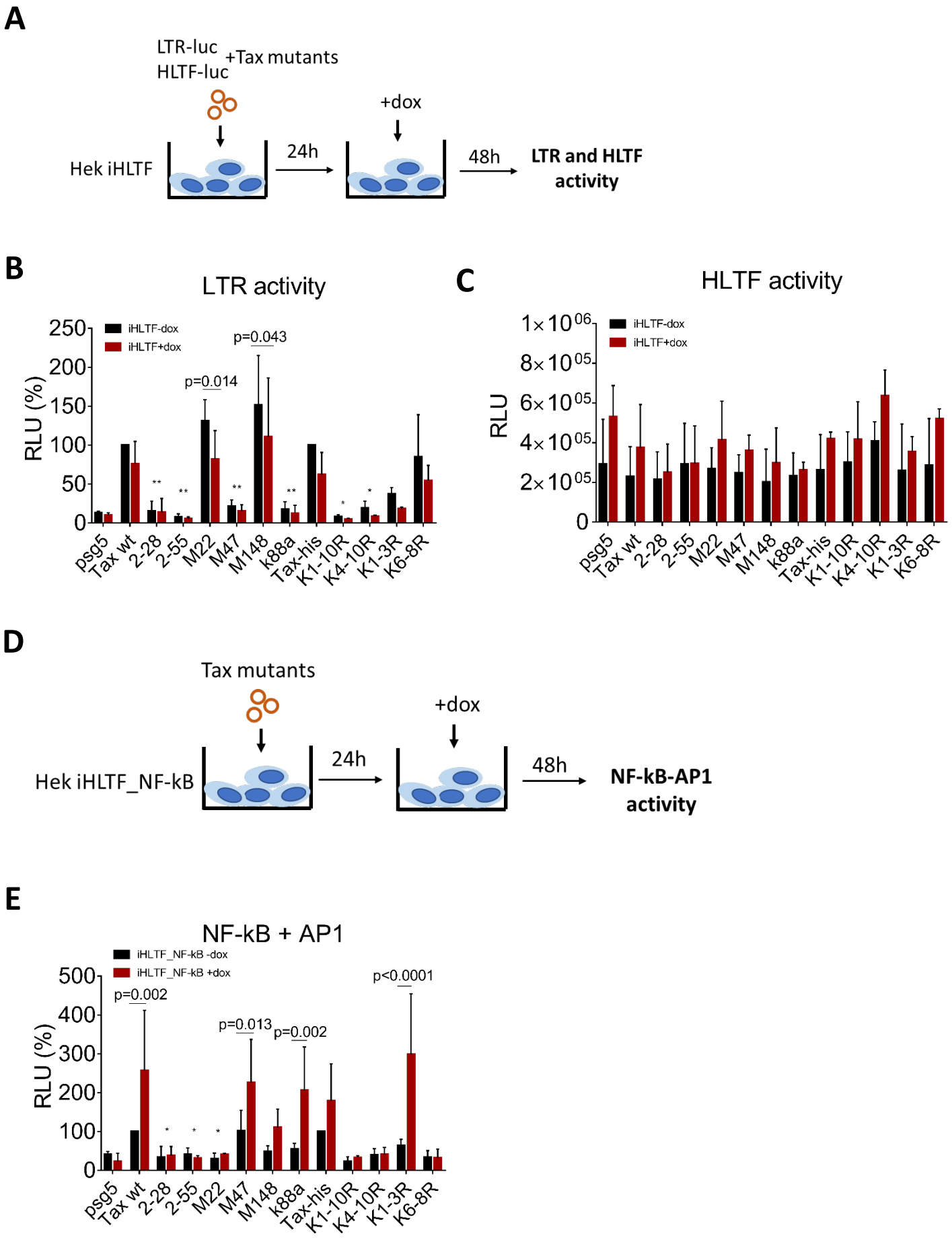

*Figure 17: **Effects of Tax mutants on NF-κB, LTR and HLTF promoter**. **(A)** Established HekiHLTF cell lines were transfected with the different Tax mutants and doxycycline-inducible LTR-Luc or HLTF-Luc plasmids. The activity of the LTR and HLTF promoter was assessed by quantifying the luciferase activity 48 hours after induction. Luciferase activity was measured in relative luminescence units (RLU) **(B)** for LTR and **(C)** for the HLTF promoter. pSG5 cells were used as control. **(D)** Established HekiHLTF_NF-κB cell lines were transfected with the different Tax mutants and induced with doxycycline. NF-κB activity was assessed by quantifying luciferase activity 48 hours after induction. **(E)** Luciferase activity was measured in relative luminescence units (RLU), pSG5 cells were used as control. Activity of Tax_WT was set to 100%. The statistical significance was determined by t test and by a single-step Turkey's multiple comparisons test: p<0.05 (*), p<0.01 (**) or p<0.001 (***).*

5) Effects of HLTF mutants

The established cell lines (HekiHLTF, HekMut_RING, HekMut_HIRAN) were transfected with luciferase reporters (LTR-Luc or HLTF-Luc or NF-κB-Luc) and pSG5 or Tax_WT. LTR, and HLTF promoter activities, and NF-κB signalling were analyzed 48h after induction of HLTF expression with doxycycline (**Figure 18A**).

Transfection of the LTR-Luc reporter and the Tax_WT plasmid increased luciferase activity compared to the pSG5 control confirming that Tax transactivates the LTR. However, no significant difference in luciferase activity was observed in HekiHLTF, HekMut_RING, HekMut_HIRAN. None of the HLTF mutants show a reduction or increase in luciferase activity suggesting that no HLTF mutant influences the LTR activation (**Figure 18B**).

Tax and HLTF mutants had no effect on HLTF promoter activation. Indeed, there was no difference in the luciferase signal observed between mutants transfected with the pSG5 plasmid and the Tax-WT plasmid, indicating that neither Tax nor HLTF mutants influence HLTF promoter activation (**Figure 18C**).

Experiments to observe the effect of Tax and HLTF mutants on the NF-κB activation pathway revealed an increase of luciferase activity in cells transiently transfected with the Tax_WT plasmid compared to pSG5 indicating that Tax strongly transactivates NF-κB. However, no difference in luciferase activity was observed between induced and uninduced cells transiently transfected with Tax_WT plasmid. No HLTF mutants show reduced or increased luciferase activity suggesting that no HLTF mutant is defective in NF-κB activation (**Figure 18D**).

The established cell lines HekiTax, HekiHLTF, HekiTaxiHLTF were transfected with the doxycycline inducible NF-κB-Luc plasmid. NF-κB activity was assessed by quantifying luciferase activity 48 hours after induction. In these conditions, HLTF has no effect on NF-κB signaling. In contrast, induction of Tax increased NF-κB-dependent luciferase activity. Simultaneous induction of Tax and HLTF increased the luciferase signal (**Figure 18E**). However, no synergistic effect was observed in contrast to the results obtained for established doxycycline-inducible NF-κB-AP-1-Luc lines (**Figure 15B**).

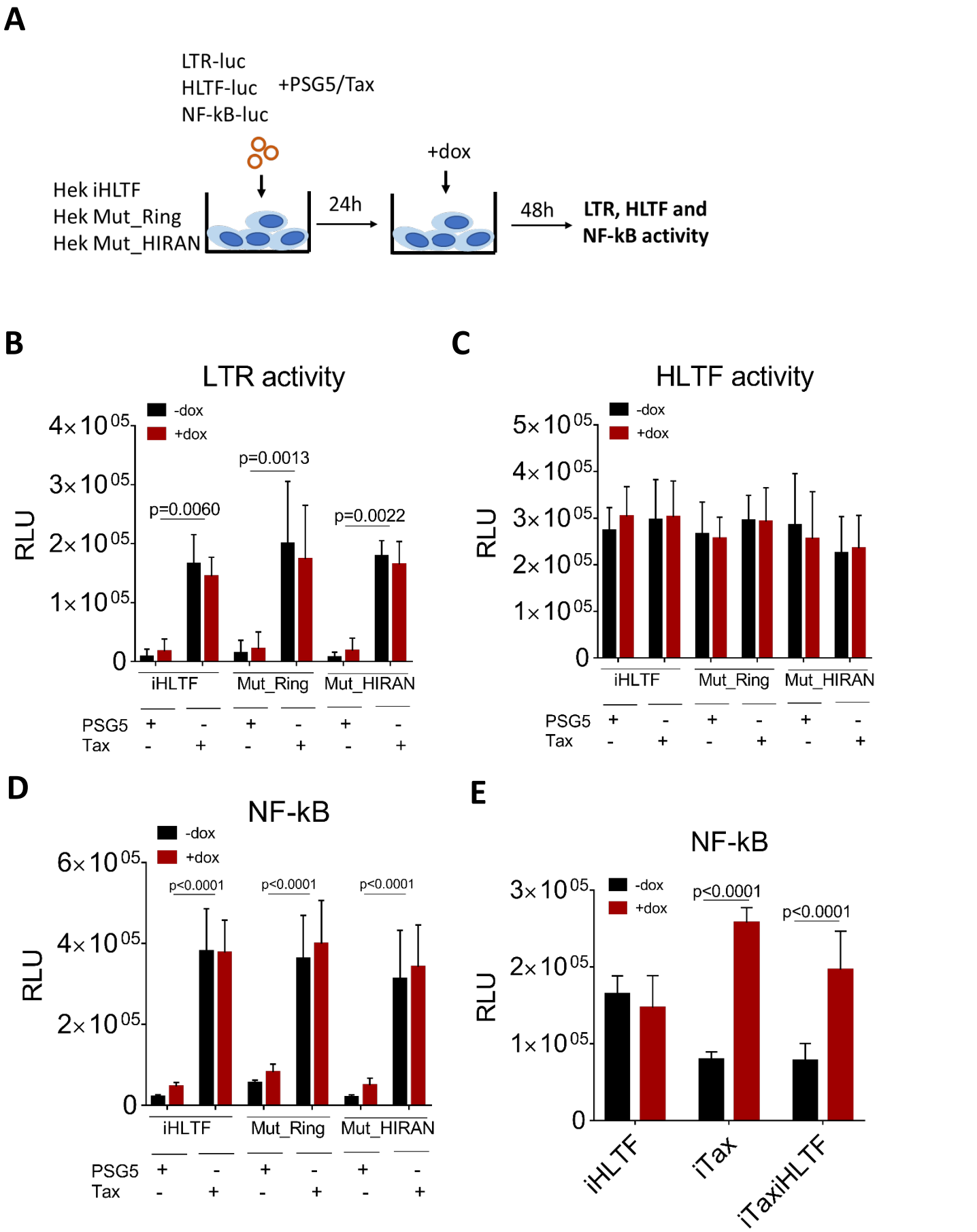

Figure 18: ***Effects of HLTF mutants on NF-κB, LTR and HLTF promoter****. **(A)** Established HekiHLTF, Hek_Mut_RING, Hek_Mut_HIRANcell lines were transfected with the different Tax mutants and LTR-Luc or HLTF-Luc plasmids. The activity of the LTR and HLTF promoter was assessed by quantifying the luciferase activity 48 hours after induction. Luciferase activity was measured in relative luminescence units (RLU) **(B)** for LTR of HLTF mutants, **(C)** for the HLTF promoter of HLTF mutants, **(D)** for NF-κB of HLTF mutants and **(E)** NF-κB of established cell lines HekiTax, HekiHLTF and HekiTaxiHLTF. Activity of iHLTF was set to 100%. The statistical significance was determined by t test.*

V) Discussion

The objective of this master thesis was to evaluate the effect of Tax and HLTF on LTR and HLTF promoter activities as well as on NF-κB signaling.

The results obtained show that:

⇒ Tax strongly induces NF-κB signalling and LTR promoter activity (CREB pathway).

⇒ Tax mutants 2-28, 2-55, M47, K88A, K1-3R, K1-10R, K4-10R are defective in LTR activation.

⇒ Tax mutants 2-28, 2-55, M22, M148, K1-10R, K6-8R, K4-10R are defective in NF-κB activation.

⇒ Mutant and wild-type Tax have no effect on HLTF promoter activity.

⇒ Co-expression of HLTF mutants and Tax has effect neither on NF-κB signaling nor on LTR and HLTF promoter activities.

⇒ A synergistic effect of Tax and HLTF in NF-κB activation is observed in cells permanently transduced with the NF-κB -AP-1-Luc but is absent in cells transiently transfected with NF-κB-Luc plasmid.

1) Tax mutants defective in NF-κB activation

In the NF-κB activation pathway, Tax ubiquitination is essential for the assembly of active IKK complexes and translocation of RelA into the nucleus[63].
Our data indicate that HLTF induction has no influence on NF-κB activation. The results show that the level of NF-κB activation upon HLTF induction increases in the presence of Tax and its mutants (Tax wt, M22, M47, K88a, Tax-Hix, K1-3R) compared to HLTF induction alone (**Figure 17E**) except for mutants 2-28, 2-55, M148, K1-10R, K6-8R and K4-10R.

The inability of mutants 2-28, 2-55 to activate NF-κB could be due to the deletion of part of the zinc interaction domain or the NLS. The ankyrin repeat motif (30-33 amino acids) shared by the seven IκB proteins responsible for interaction with NF-κB has been shown to be a central domain functioning by binding to RHDs that mask the NLS (Nuclear Localization Signal) of NF-κB proteins. The masked NLS becomes inactive resulting in the sequestration of the NF-κB family in the cytoplasm, which thus becomes unable to migrate into the nucleus and thus induce gene transcription[88,94,96,98]. A hypothesis that the mutation in the Tax NLS prevents the translocation of NF-κB dimers to the nucleus and thus induces NF-κB activation could be established.

Studies have shown that the K1-10R, K6-8R and K4-10R mutants are defective in NF-κB activation[118]. However, results shows that K1-10R, K6-8R and K4-10R are not significantly deficient in NF-κB activation in HekiHLTF cells despite a lower luciferase activity signal (**Figure 17E**). This could be explained by the low repetition rate (3 tests). Indeed, performing more repeats could be consistent with the literature.

Only the K1-3R mutant retains full activity and overactivate NF-κB. The K1-3R mutant has been shown not to be defective in NF-κB activation[118].

The central and C-terminal lysine (K4-K10) have been shown to be involved in Tax ubiquitination[63,118,119]. Indeed, one study demonstrated the importance of lysines 6, 7, 8 and more particularly 7 and 8 which affect the formation of the NF-κB/DNA complex in the activation of the NF-κB pathway[118].

As mentioned in the introduction, Tax activation of the canonical and non-canonical NF-κB signaling pathway requires Tax binding to NEMO/IKK-γ and the IKK complex[116]. Tax has been shown to physically interact with IKK-γ via the two putative leucine zipper (LZ) motifs in IKK-γ located between amino acid residues 100 - 140 and 312 - 340. The leucine-rich sequence located between amino acid residues 105 - 141 is the Tax region important for Tax binding to IKK-γ[78].The localization of the double missense mutation in Tax (T130A and L131S = M22) (**Figure 7**) results in an inability of the Tax mutant M22 to bind to NEMO. The inability of Tax to bind to NEMO results in the failure of NF-κB activation[116].

Tax's missense mutation of glycine (148) to valine generates the M148 mutant in the NF-κB activation and p300-binding domain. This mutation in the NF-κB activation domain would therefore prevent transactivation of the NF-κB pathway by the Tax M148 mutant. A study shows that Tax mutants capable of activating NF-κB are localized in CBP region of Tax protein but not in p300 while Tax mutants capable of activating LTR are localized in p300 region of Tax protein but not in CBP[77]. The inability of M148 to activate NF-κB can be correlated with

its mutation position in p300 region of tax protein as well as in the activation domain of NF-κB.

The localization of K6-8R and K4-10R (**Figure 7**) gives them the possibility to bind to IKK-γ without inducing transactivation of the NF-κB pathway.

Tax has been shown to interact with PP2A (serine/threonine protein phosphatase 2A), the inhibitor of IKK. Mutants unable to bind PP2A (serine/threonine protein phosphatase 2A), whether they can bind IKK-γ or not, lead to an inactivation of the NF-κB pathway[120].

Therefore, it could be concluded that the inability of the K6-8R and K4-10R mutants to induce transactivation of the NF-κB pathway is probably due to their inability to bind to PP2A even though they would appear to bind to IKK-γ.

Western blot results also show that Tax mutants unable to induce NF-κB have lower levels of Tax p compared to Tax-WT. However, despite the 58.5% reduction in NF-κB activity for the M148 mutant, it has a high level of Tax protein (1.30 intensity) compared to Tax_WT (0.53 intensity) (**Figure 16F**).

In summary, the Tax mutants identified as defective in NF-κB pathway activation correspond to the literature. The M148 mutant has been described in the literature as defective in NF-κB activation without mentioning the rate of reduction, but our results show that it alters NF-κB activation with a 58.5% reduction. Our experiments allow us two mutants 2-28, 2-55 which have not been described in the literature.

2) Tax mutants defective in LTR activation

It has been demonstrated that Tax activation of the HTLV-1 LTR is mediated by constitutively expressed cellular factors that bind to cAMP response elements (CREs) present in the 21-bp activators of the LTR[121]. Therefore, a mutation in the CREB interaction domain of Tax could affect LTR promoter activation as well as CREB activation.

The 2-28 and 2-55 mutants located in the CREB activation domain would appear to affect the interaction of Tax with CREB leading to inactivation of the LTR promoter. Indeed, mutants 2-28 and 2-55 resulted in a significant deleterious effect on the interaction of Tax with CREB.

The double missense mutation of Tax (L319R and L320S: M47) was made in the CREB interaction domain of Tax and in the activation domain for transcription. This mutation in Tax (M47) would prevent the interaction of Tax with CREB leading to an inability to activate the LTR promoter as well as CREB.

Given the results, it is possible to draw a hypothesis according to which any mutation carried out in the CREB interaction domain of Tax would lead to a failure to activate the LTR promoter and therefore a failure of Tax to induce transactivation of the CREB pathway. This hypothesis would explain the inability of mutants 2-28, 2-55, M47, K1-10R, and K4-10R, to induce LTR promoter activation (**Figure 17B**).

On the other hand, the K88A and K1-3R mutations were made in the Tax interaction domain with CBP/p300. It was shown that K88A is unable to interact with CBP/p300 and to activate the transcription of the long terminal repeat (LTR)[122]. It has also been shown that the inability of K1-3R to activate CREB and thus the long terminal repeat (LTR) transcript is probably due to the mutation in the CBP/p300 binding domain[118]. The inability of these two mutants to activate the LTR could therefore be explained by the reported role of all amino acids (81-95) contained in this CBP/p300 binding region with Tax.

3) Tax mutants defective in LTR and NF-κB

The results obtained show that the mutants 2-28, 2-55, K1-10R, K4-10R are defective to both NF-κB activation and LTR (**Figure 17B-E**).

A study has shown that K1-10R, K4-10R are defective in the LTR and NF-κB activation pathway, probably due to a structural or folding defect[118]. This structural or folding defect hypothesis could also explain why the 2-28, 2-55 mutants are both defective in LTR and NF-κB activation.

4) Tax does not activate the HLTF promoter

Studies of the effect of Tax mutants or HLTF mutants on HLTF promoter activation show no difference in HLTF promoter activation between induced and non-induced cells suggesting that Tax and HLTF do not transactivate the HLTF promoter (**Figure 17C-18C**).

All the results obtained therefore show that neither Tax, nor HLTF influence the activation of the HLTF promoter (**Figure 17C- 18C**).

These results show that despite the demonstrated interaction between Tax and HLTF, the induction of one or both proteins do not influence the activation of the HLTF promoter.

Other Tax mutants such as K7-8R, K4-8R, K8R, K7R as well as those described in *Smith, M. R. et al*. can also be used to assess HLTF promoter activity. However, if none of these mutants show an effect, then it could be concluded that none of the Tax mutants are likely to activate

the HLTF promoter. However, if any of these mutants are found to activate the HLTF promoter, it will be necessary to determine what type of mutations and what element in Tax are required to transactivate the HLTF promoter.

These results show that HLTF does not transactivate its own promoter. However, these results could be used to determine whether HLTF transactivates its own promoter under other conditions and to establish what conditions, if any, are necessary for this to occur.

5) Effect of simultaneous Tax and HLTF induction on NF-κB

Tax and HLTF have been shown to interact together[123].

Analysis of the effects of the established cell lines HekiTax, HekiHLTF, HekiTaxiHLTF transduced with the NF-κB-AP-1-Luc plasmid on NF-κB activation showed a synergistic effect of NF-κB pathway activation when Tax and HLTF were induced simultaneously.

One study demonstrated that the ubiquitin UBE4B ubiquitinates Tax and increases Tax-mediated NF-κB activation[124]. It could be assumed that during the infectious life cycle of HTLV-1, after the production of viral proteins, part of Tax could be involved in the NF-κB activation pathway. Tax would interact directly with HLTF, which would behave like an E3 ubiquitin ligase thanks to its RING domain characteristic of E3 ubiquitin ligases. HLTF would therefore interact directly with Tax and ubiquitinate it to activate the NF-κB signaling pathway mediated by Tax. Tax could also be K63-, K48-polyubiquitinated.

The polyubiquitination of Tax would favor its direct interaction with NEMO/IKK-γ, thus allowing the recruitment of the IKK complex. This recruitment would lead to the phosphorylation and degradation of IκB by the proteasome as well as the translocation of NF-κB dimers (RelA/p50, RelB/p52) to the nucleus. The NF-κB dimers (RelA/p50, RelB/p52) induce the expression of NF-κB genes leading to the activation of the NF-κB pathway.

The ubiquitin ligase role of HLTF as well as its interaction with Tax could therefore explain the synergistic effect observed during the simultaneous induction of Tax and HLTF (**Figure 15B**).

To verify this hypothesis, a co-immunoprecipitation could be performed to identify whether Tax is ubiquitinated (mono- or polyubiquitinated) or not. For this purpose, Tax protein should be precipitated in HLTF-induced and non-induced cells. Tax immunoprecipitates should be analyzed by Western blotting using anti-K63 or anti-K48 antibodies. If no difference in polyubiquitination of Tax is observed in the co-immunoprecipitation analysis, then the synergistic effect is not due to the role of HLTF ubiquitin ligase.

In addition to co-immunoprecipitation, other mutations (deletion, substitution) in the other part of RING domain could be performed to determine which part of domain of RING is essential for the characteristic ligase activity of the RING domain.

This synergistic effect is only observable for cell lines transduced with the NF-κB-AP-1-Luc plasmid (**Figure 15B**) but not with cell lines transiently transfected with the NF-κB-Luc plasmid (**Figure 18E**).

The results obtained make it possible to list several plausible hypotheses on the synergistic effect due to the simultaneous induction of Tax and HLTF:

- ⇒ The synergistic effect is due to the presence of the activator protein AP-1 which is a transcription factor. To reject this hypothesis, the experiments should be repeated by transiently transfecting the cell lines with an AP-1-reporter plasmid. If the results show a synergistic effect of the simultaneous induction of Tax and HLTF, then the synergistic effect observed is indeed due to AP-1. However, if no synergistic effect is observed, it could mean that upon simultaneous induction of Tax and HLTF, both proteins need AP-1 as an intermediary to induce a synergistic effect of NF-κB pathway activation.
- ⇒ The synergistic effect could be because the cell lines were permanently transduced with the NF-κB-AP-1-Luc plasmid but transiently transfected with the NF-κB-Luc plasmid. To remove this doubt, it would be wise to establish cell lines transduced with the NF-κB-Luc plasmid. If no synergistic effect can be observed after the transduction of cells with the NF-κB-Luc plasmid, the effect is not due to whether the plasmid is integrated (permanent) or not (transient) but probably to the composition of the plasmids used.

VI) Conclusion

The aim of this thesis was to evaluate the impact of Tax and HLTF mutants on the activation of NF-κB, LTR and the HLTF promoter.

The results obtained reveal that, upon simultaneous induction of Tax and HLTF, a synergistic effect on NF-κB activation is observed for cells transduced with the NF-κB-AP-1-Luc plasmid but not for cells transiently transfected with the NF-κB-Luc plasmid, probably due to the presence of AP-1. The lack of synergistic effect in cells transiently transfected with NF-κB-Luc plasmid would probably explain the lack of effect of HLTF mutants on NF-κB activation.

The results also reveal that no activation pathway is impacted by HLTF mutants.

To date, no research on the effect of HLTF mutants on activation pathways has been conducted. It is, therefore, possible to further investigate this mechanism by creating new mutants for HLTF and finding out whether the synergistic effect on NF-κB activation due to the simultaneous induction of Tax and HLTF is indeed due to AP-1 or to the method used for the integration of the plasmid of interest (permanent transduction or transient transfection).

VII) References

1 Romanelli, M. G. *et al. Front. Microbiol.* 4, 271 (2013)

2 Hoshino, H. *Front. Microbiol.* 3, 222 (2012)

3 Martinez, M. P. *et al. Retrovirology 2019 161* 16, 1–12 (2019)

4 Abbas, A. L. *et al. AIDS Res. Hum. Retroviruses* 36, 967–968 (2020)

5 de Thé, G. *et al. AIDS Res. Hum. Retroviruses* 9, 381–6 (1993)

6 Gonçalves, D. U. *et al. Clin. Microbiol. Rev.* 23, 577 (2010)

7 Gessain, A. *et al. Med. Mal. Infect.* 24, 543–547 (1994)

8 Matsuoka, M. *Retrovirology* 2, 1–13 (2005)

9 Matsuura, E. *et al. J. Neuroimmune Pharmacol. 2010 53* 5, 310–325 (2010)

10 Gessain, A. *et al. Front. Microbiol.* 3, 388 (2012)

11 Gessain, A. *Bull. la Soc. Pathol. Exot.* 104, 167–180 (2011)

12 Harhaj, E. W. *et al. FEBS J.* 285, 3324 (2018)

13 Gonçalves, D. U. *et al. Clin. Microbiol. Rev.* 23, 577–589 (2010)

14 Gessain, A. *et al. Front. Microbiol.* 3, 388 (2012)

15 Yoshida, M. *Oncogene 2005 2439* 24, 5931–5937 (2005)

16 Phillips, A. A. *et al. Curr. Hematol. Malig. Rep.* 13, 300–307 (2018)

17 HINO, S. *Proc. Japan Acad. Ser. B* 87, 152–166 (2011)

18 Ureta-Vidal, A. *et al. Int. J. Cancer* 82, 832–836 (1999)

19 Pique, C. *et al. Front. Microbiol.* 3, 378 (2012)

20 Khabbaz, R. F. *et al. N. Engl. J. Med.* 326, 375–380 (1992)

21 Brites, C. *et al. AIDS Rev.* 11, 8–16 (2008)

22 Aghajanian, S. *et al. Front. Microbiol.* 11, 614940 (2020)

23 Katsuya, H. *et al. Cell Rep.* 29, 724-735.e4 (2019)

24 Franchini, G. *Blood* 86, 3619–39 (1995)

25 Panfil, A. R. *et al. Front. Cell. Infect. Microbiol.* 10, 813 (2020)

26 Koralnik, I. J. *et al. Med. Sci.* 89, 8813–8817 (1992)

27 Kannian, P. *et al. Viruses* 2, 2037 (2010)

28 Ciminale,', V. *et al. J. Virol.* 1737–1745 (1992)

29 Felber, B. K. *et al. Science (80-.).* 229, 675–679 (1985)

30 ALCOVER, J. A. *et al. Tropics* 10, 10 (2016)

31 Kashanchi, F. *et al. Oncogene 2005 2439* 24, 5938–5951 (2005)

32 Grassmann, R. *et al. J. Virol.* 66, 4570–4575 (1992)

33 Robek, M. D. *et al. J. Virol.* 73, 4856–4865 (1999)

34 Basbous, J. *et al. J. Biol. Chem.* 278, 43620–43627 (2003)

35 Thébault, S. *et al. FEBS Lett.* 562, 165–170 (2004)

36 Lemasson, I. *et al. J. Virol.* 81, 1543–1553 (2007)

37 Gaudray, G. *et al. J. Virol.* 76, 12813–12822 (2002)

38 Ghez, D. *et al. J. Virol.* 80, 6844–6854 (2006)

39 Franchini, G. *et al. Leuk. Res.* 9, 1305–1314 (1985)

40 Panfil, A. R. *et al. Curr. Opin. Virol.* 20, 40–46 (2016)

41 Enose-Akahata, Y. *et al. Front. Microbiol.* 8, 2563 (2017)

42 Kannian, P. *et al. J. Virol.* 86, 3757–3766 (2012)

43 Nejmeddine, M. *et al. Viruses 2010, Vol. 2, Pages 1427-1447* 2, 1427–1447 (2010)

44 Bard, . E *et al. 24. A. F. Fanning, A. J. Weav. Paleoceanogr* 345, 962 (1990)

45 Gross, C. *et al. Viruses 2016, Vol. 8, Page 74* 8, 74 (2016)

46 Gross, C. *et al. Viruses* 8, 74 (2016)

47 Van Prooyen, N. *et al. Proc. Natl. Acad. Sci. U. S. A.* 107, 20738–20743 (2010)

48 Pais-Correia, A. M. *et al. Nat. Med. 2009 161* 16, 83–89 (2009)

49 Forlani, G. *et al. Int. J. Mol. Sci.* 22, 8001 (2021)

50 Cook, L. *et al. Curr. Opin. Virol.* 26, 125–131 (2017)

51 Ghez, D. *et al. J. Virol.* 80, 6844–6854 (2006)

52 Kusuhara, K. *Fukuoka Igaku Zasshi* 92, 385–392 (2001)

53 Martin, J. L. *et al. Viruses 2016, Vol. 8, Page 31* 8, 31 (2016)

54 Fogarty, K. H. *et al. Viruses* 3, 770–793 (2011)

55 Satou, Y. *et al. Proc. Natl. Acad. Sci. U. S. A.* 103, 720–725 (2006)

56 Matsuoka, M. *Retrovirology* 2, 1–13 (2005)

57 Yasunaga, J. I. *Front. Microbiol.* 11, 979 (2020)

58 Muñoz, E. *et al. J. Virol.* 68, 8035–44 (1994)

59 Vandermeulen, C. *et al. PLOS Pathog.* 17, e1009919 (2021)

60 Takeda, S. *et al. Int. J. Cancer* 109, 559–567 (2004)

61 Mohanty, S. *et al. PLOS Pathog.* 16, e1008504 (2020)

62 Zhao, T. *et al. Arch. Virol. 2014 1597* 159, 1849–1856 (2014)

63 Lodewick, J. *et al. Viruses* 3, 829–857 (2011)

64 Bex, F. *et al. Mol. Cell. Biol.* 18, 2392 (1998)

65 Harhaj, E. W. *et al. IUBMB Life* 57, 83–91 (2005)

66 Boxus, M. *et al. Retrovirology* 5, 1–24 (2008)

67 Ng, P. W. *et al. Oncogene* 20, (2001)

68 Wagner, S. *et al. Science* 262, 395–9 (1993)

69 Fochi, S. *et al. Front. Microbiol.* 9, 285 (2018)

70 Zhao, T. *Viruses 2016, Vol. 8, Page 34* 8, 34 (2016)

71 Taniguchi, Y. *et al. Retrovirology* 2, 64 (2005)

72 Kuo, Y. L. *et al. EMBO J.* 25, 1741 (2006)

73 Alefantis, T. *et al. J. Biol. Chem.* 278, 21814–21822 (2003)

74 Kimzey, A. L. *et al. J. Biol. Chem.* 274, 34226–34232 (1999)

75 Semmes, O. J. *et al. J. Virol.* 69, 1827 (1995)

76 Lenzmeier, B. A. *et al. Mol. Cell. Biol.* 18, 721 (1998)

77 Oise Bex, F. *et al. Mol. Cell. Biol.* 18, 2392–2405 (1998)

78 Xiao, G. *et al. J. Biol. Chem.* 275, 34060–34067 (2000)

79 Yasuma, K. *et al. PLOS Pathog.* 12, e1005372 (2016)

80 Dhont, L. *et al. Cell. Mol. Life Sci.* 73, 129–145 (2016)

81 Arcolia, V. *et al. BMC Cancer* 14, 1–12 (2014)

82 Hishiki, A. *et al. J. Biol. Chem.* 290, 13215 (2015)

83 Unk, I. *et al. DNA Repair (Amst).* 9, 257–267 (2010)

84 Hibi, K. *et al. Int. J. Cancer* 104, 433–436 (2003)

85 Moinova, H. R. *et al. Proc. Natl. Acad. Sci.* 99, 4562–4567 (2002)

86 Yan, J. *et al. Proc. Natl. Acad. Sci. U. S. A.* 116, 9568–9577 (2019)

87 Nightingale, K. *et al. Cell Host Microbe* 24, 447-460.e11 (2018)

88 Trask, O. J. *Assay Guidance Manual* (Eli Lilly & Company and the National Center for Advancing Translational Sciences, 2004)

89 Hayden, M. S. *et al. Genes Dev.* 26, 203–234 (2012)

90 The NF-κB Signaling Pathway - Creative Diagnostics https://www.creative-diagnostics.com/The-NF-κB-Signaling-Pathway.htm (accessed Jun 30, 2022).

91 Hua, X. *et al. Gene Expr.* 7, 233 (1999)

92 Zinatizadeh, M. R. *et al. Genes Dis.* 8, 287–297 (2021)

93 Pujari, R. *et al. PLOS Pathog.* 11, e1004721 (2015)

94 Oeckinghaus, A. *et al. Cold Spring Harb. Perspect. Biol.* 1, a000034–a000034 (2009)

95 Mukherjee, S. P. *et al. Proc. Natl. Acad. Sci. U. S. A.* 113, 6212–6217 (2016)

96 Albensi, B. C. *Front. Cell Dev. Biol.* 7, 154 (2019)

97 Wu, J. *et al. Front. Immunol.* 9, (2018)

98 Zheng, C. *et al. Cell Res.* 21, 183 (2011)

99 Janeway, C. A. *et al. Annu. Rev. Immunol* 20, 197–216 (2002)

100 Gilmore, T. D. *Oncogene* 18, 6842–6844 (1999)

101 Baldwin. *Annu. Rev. Immunol.* 14, 649–83 (1996)

102 NF-κB Signaling | Cell Signaling Technology https://www.cellsignal.at/pathways/nfkb-signaling-pathway (accessed Jul 2, 2022)(2009)

103 Muñoz, E. *et al. J. Virol.* 68, 8035–8044 (1994)

104 Blank, V. *et al. Trends Biochem. Sci.* 17, 135–140 (1992)

105 Sun, S.-C. *et al. Oncogene* 18, 6948–6958 (1999)

106 Petropoulos, L. *et al. Virology* 225, 52–64 (1996)

107 Arima, N. *et al. J. Virol.* 65, 6892–6899 (1991)

108 Pepin, N. *et al. Virology* 204, 706–716 (1994)

109 Kfoury, Y. *et al. Advances in Cancer Research* 113, (Elsevier Inc., 2012)

110 Hirai, H. *et al. Proc. Natd. Acad. Sci. USA* 91, (1994)

111 Chen, Z. J. *et al. Cell* 84, 853–862 (1996)

112 Wu, X. *et al. EMBO Rep.* 8, 510–515 (2007)

113 Yu, Q. *et al. Biochem. Biophys. Res. Commun.* 365, 189–194 (2008)

114 Hirai, H. *et al. Proc. Natl. Acad. Sci. U. S. A.* 91, 3584–3588 (1994)

115 Chu, Z. L. *et al. J. Biol. Chem.* 274, 15297–15300 (1999)

116 Harhaj, E. W. *et al. J. Biol. Chem.* 274, 22911–22914 (1999)

117 Pomerantz, J. L. *et al. Mol. Cell* 10, 693–695 (2002)

118 Nasr, R. *et al. Blood* 107, 4021–4029 (2006)

119 Chiari, E. *et al. J. Virol.* 78, 11823 (2004)

120 Fu, D. X. *et al. J. Biol. Chem.* 278, 1487–1493 (2003)

121 Smith, M. R. *et al. Genes Dev.* 4, 1875–1885 (1990)

122 Wencker, M. *et al. J. Virol.* 81, 301–308 (2007)

123 Beauvois, A. (2020)

124 Mohanty, S. *et al. PLOS Pathog.* 16, e1008504 (2020)

125 Unk, I. *et al. Proc. Natl. Acad. Sci.* 105, 3768–3773 (2008)

VIII) Annexes

Annex I: References of cell lines

Cells lines	References
Hek293T	ATCC CRL-157

Annex II: HLTV-1 Tax protein sequence exported from Uniprot

Tax Wild-Type	M A H F P G F G Q S L L F G Y P V Y V F G D C V Q G D W C P	30
	I S G G L C S A R L H R H A L L A T C P E H Q I T W D P I D	60
	G R V I G S A L Q F L I P R L P S F P T Q R T S K T L K V L	90
	T P P I T H T T P N I P P S F L Q A M R K Y S P F R N G Y M	120
	E P T L G Q H L P T L S F P D P G L R P Q N L Y T L W G G S	150
	V V C M Y L Y Q L S P P I T W P L L P H V I F C H P G Q L G	180
	A F L T N V P Y K R I E E L L Y K I S L T T G A L I I L P E	210
	D C L P T T L F Q P A R A P V T L T A W Q N G L L P F H S T	240
	L T T P G L IW T F T D G T P M I S G P C P K D G Q P S L V	270
	L Q S S S F I F H K F Q T K A Y H P S F L L S H G L I Q Y S	300
	S F H S L H L L F E E Y T N I P I S L L F N E K E A D D N D	330
	H E P Q I S P G G L E P P S E K H F R E T E V	353